Liming effects on microbial carbon use efficiency and its potential consequences for soil organic carbon stocks

Julia Schroeder, Claudia Dămătîrcă, Tobias Bölscher, Claire Chenu, Lars Elsgaard, Christoph C Tebbe, Laura Skadell, Christopher Poeplau

Soil Biology and Biochemistry 191 (2024) 109342

Contents lists available at ScienceDirect

Soil Biology and Biochemistry

journal homepage: www.elsevier.com/locate/soilbio

Liming effects on microbial carbon use efficiency and its potential consequences for soil organic carbon stocks

Julia Schroeder [a,*], Claudia Dămătîrcă [b,1], Tobias Bölscher [c], Claire Chenu [c], Lars Elsgaard [d], Christoph C. Tebbe [e], Laura Skadell [a], Christopher Poeplau [a]

[a] Thünen Institute of Climate-Smart Agriculture, Bundesallee 68, 38116, Braunschweig, Germany
[b] University of Turin, Department of Agricultural, Forest and Food Sciences, Largo Paolo Braccini 2, 10095, Grugliasco, TO, Italy
[c] Université Paris-Saclay, INRAE, AgroParisTech, UMR EcoSys, 22 Place de l'Agronomie, 91120, Palaiseau, France
[d] Aarhus University, Department of Agroecology, Blichers Allé 20, 8830, Tjele, Denmark
[e] Thünen Institute of Biodiversity, Bundesallee 65, 38116, Braunschweig, Germany

ARTICLE INFO

Keywords:
Climate change mitigation
Agricultural soil
Organic C inputs
Isotopic labelling
Microbial soil carbon
Long-term field experiment (LTE)

ABSTRACT

Climate-smart agriculture aims amongst others at protecting and increasing soil organic carbon (SOC) stocks. The allocation of metabolised carbon (C) between soil microbial growth and respiration, i.e. C use efficiency (CUE) is crucial for SOC dynamics. We hypothesised that raising soil pH would alleviate CUE-limiting conditions and that liming could thus increase CUE, thereby supporting SOC accrual. This study investigated whether CUE can be manipulated by liming and how this might contribute to SOC stock changes. The effects of liming on CUE, microbial biomass C, abundance of microbial domains, SOC stocks and OC inputs were assessed for soils from three European long-term field experiments. Field control soils were additionally limed in the laboratory to assess immediate effects. The shift in soil pH_{H2O} from 4.5 to 7.3 with long-term liming reduced CUE by 40 %, whereas the shift from 5.5 to 8.6 and from 6.5 to 7.8 was associated with increases in CUE by 16 % and 24 %, respectively. The overall relationship between CUE and soil pH followed a U-shaped (i.e. quadratic) curve, implying that in agricultural soils CUE may be lowest at $pH_{H2O} = 6.4$. The immediate CUE response to liming followed the same trends. Changes in CUE with long-term liming contributed to the net effect of liming on SOC stocks. Our study confirms the value of liming as a management practice for climate-smart agriculture, but demonstrates that it remains difficult to predict the impact on SOC stocks due its complex effects on the C cycle.

1. Introduction

An important part of climate-smart agriculture is to preserve and increase carbon (C) stocks in soils. To obtain soil organic C (SOC) accrual, management needs to allow more C to enter and remain in the soil than is lost. This balance is strongly determined by soil microbial C processing (Schimel and Schaeffer, 2012), which depends on the quantity and quality of OC inputs, distribution and accessibility or physicochemical protection, i.e. stabilisation, and the microbial community (Conant et al., 2011). During the metabolic breakdown of soil organic matter, C is lost from the soil by respiration as CO_2. Although counterintuitive, decomposition could, however, help to stabilise C and thus support C storage in soil, because microbial-derived compounds and necromass eventually interact with mineral surfaces and stabilise in form of mineral-associated organic matter (MAOM) (Liang et al., 2017, 2019). Here, microbial carbon use efficiency (CUE) represents a key control factor on the fate of organic C in soil, since it is a measure of the proportion of metabolised C being used for microbial growth or respiration (Manzoni et al., 2012). At high CUE, the relative CO_2 losses during decomposition are relatively low. Additionally, a high CUE is likely to support the *in-vivo* pathway of C stabilisation by supporting the formation of microbial biomass (C_{mic}) and eventually necromass (Liang

* Corresponding author.
E-mail addresses: julia.schroeder@thuenen.de (J. Schroeder), claudia.damatirca@cmcc.it (C. Dămătîrcă), tobias.bolscher@inrae.fr (T. Bölscher), claire.chenu@inrae.fr (C. Chenu), lars.elsgaard@agro.au.dk (L. Elsgaard), christoph.tebbe@thuenen.de (C.C. Tebbe), laura.skadell@thuenen.de (L. Skadell), christopher.poeplau@thuenen.de (C. Poeplau).
[1] Current address: Euro-Mediterranean Center on Climate Change (CMCC) Foundation, Division on Climate Change Impacts on Agriculture, Forests and Ecosystem Services (IAFES), Via Igino Garbini 51, 01100 Viterbo, Italy.

https://doi.org/10.1016/j.soilbio.2024.109342
Received 16 November 2023; Received in revised form 22 January 2024; Accepted 27 January 2024
Available online 29 January 2024

et al., 2019). Thus, a high CUE could be double beneficial for C accrual and long-term storage. Therefore, it was suggested to introduce CUE management into agroecosystem management strategies (Kallenbach et al., 2019).

Several drivers of microbial CUE have been identified such as microbial community composition (Bölscher et al., 2016; Saifuddin et al., 2019; Soares and Rousk, 2019), soil organic matter chemical composition and stoichiometry (Keiblinger et al., 2010; Manzoni et al., 2012; Sinsabaugh et al., 2016), and soil pH (Jones et al., 2019; Malik et al., 2018; Sinsabaugh et al., 2016). While it is difficult to directly manage the microbial community (Fierer and Walsh, 2023) or the quality of organic matter inputs (due to restrictions by crop rotation and agro-economic interests), adjusting soil pH could be a promising easy-to-apply option to modify microbial CUE. Recent studies suggest that CUE is sensitive to changes in soil pH induced by anthropogenic management, such as land-use change (Schroeder et al., 2022) and agricultural intensification (Malik et al., 2018). For example, a recent study found that wood-ash induced increases in soil pH following deforestation and conversion to agricultural land were the likely cause of increased CUE in subarctic soils (Schroeder et al., 2022). Further, across the United Kingdom, management intensification that shifted the soil pH above a threshold of pH = 6.2 resulted in higher CUE as compared to less intensive systems at lower soil pH (Malik et al., 2018). However, the relationship between CUE and soil pH did not appear to follow a simple positive linear relationship. Above a pH of 6.2 further increases in soil pH to slight alkalinity were not positively correlated with CUE, and when pH remained below pH = 6.2 the CUE was even negatively correlated with soil pH (Malik et al., 2018). The potential to modify CUE through manipulation of soil pH, for example by liming, and how the initial soil pH and the span of the pH shift may affect CUE response are still largely unknown.

Fig. 1 gives an overview on the underlying relationships and potential mechanisms by which liming may affect CUE and SOC-dynamics. Liming may alter CUE directly or indirectly. Direct effects of raised soil

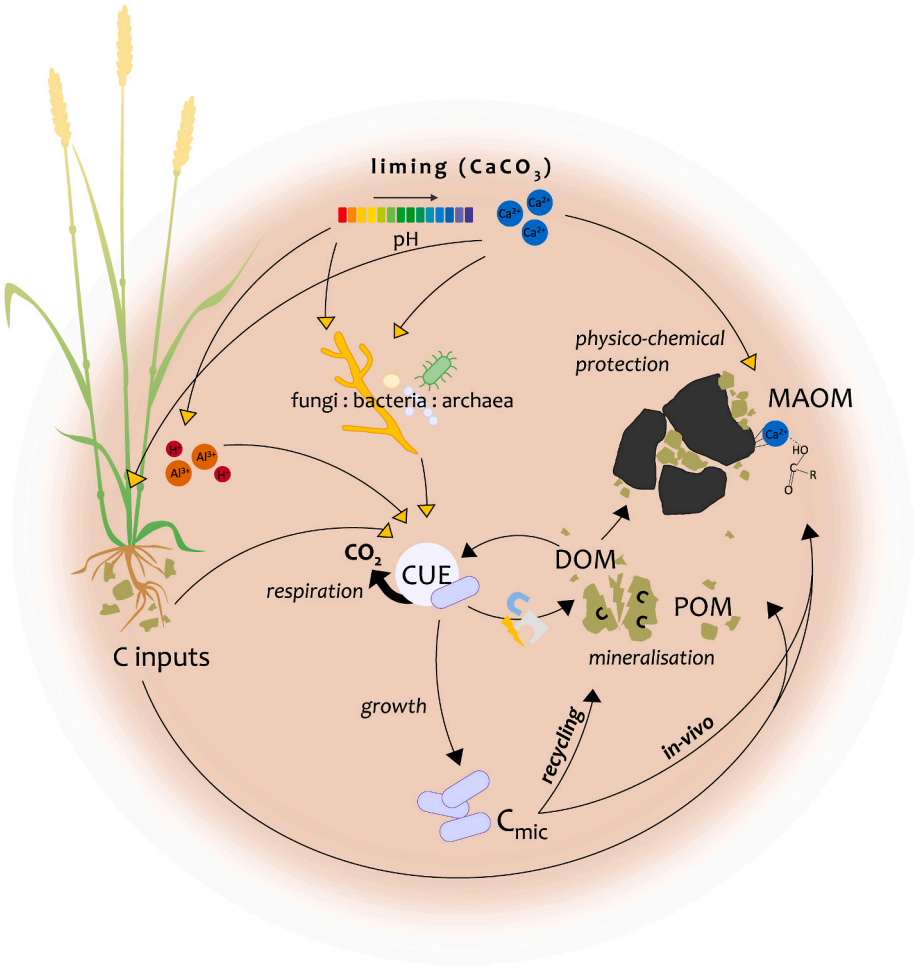

Fig. 1. Hypothesised mechanisms by which liming affects microbial carbon use efficiency (CUE) and C dynamics in agricultural soils. Effects of liming (yellow) and C fluxes (black) are displayed by arrows. Soil organic C stocks are the net sum of accumulating and depleting processes. The increase in soil pH is hypothesised to reduce Al^{3+} and/or H^+ toxicity (at low pH) and increase nutrient availability thereby promoting higher crop growth. The positive effects of Ca^{2+}-addition on soil structure will additionally benefit crop growth via improved water holding capacity. This will increase plant-derived OC inputs as particulate organic matter (POM), and dissolved organic matter (DOM), from which a part may directly form mineral-associated organic matter (MAOM). The extent to which C will be lost as CO_2 is determined by the total mineralisation and the microbial metabolic efficiency (i.e. CUE). Liming-induced shifts in CUE may alter the amount of C directed to microbial biomass C_{mic} (i.e. growth), thereby supporting OM stabilisation via formation of MAOM from necromass (i.e. *in-vivo* pathway). Liming could alter CUE i) indirectly via changes in OM quality and quantity by its effects on crop growth; ii) indirectly by affecting the microbial community composition, which is strongly determined by soil pH; and may respond to Ca^{2+} iii) directly by alleviating Al^{3+} and/or H^+ stress conditions (at low pH), thereby reducing maintenance costs. Liming may also alter OM availability by i) its effect on physicochemical protection through the addition of mineral-bridges forming Ca^{2+}, which promotes aggregation, ii) alteration of chemical equilibria affecting sorption/desorption processes. Overall, liming will affect inputs, mineralisation, microbial CUE and stabilisation of OM. Underlying mechanisms also depend on the pH range affected by liming. Liming effects on soil organic C stocks are difficult to predict, given the complexity of the processes involved.

pH could occur via a reduction of aluminium (Al^{3+}) and/or proton (H^{+}) toxicity (Jones et al., 2019), or a shift in chemical equilibria leading to altered substrate availability (Kalbitz et al., 2000). It is expected that the solubility of organic C increases with soil pH, increasing the quantity of dissolved organic C (Kalbitz et al., 2000). However, it was also shown that an increase in calcium (Ca^{2+}) concentration decreased dissolved organic C concentration in the soil solution via sorption of Ca^{2+}-bound dissolved organic C. The availability of dissolved organic C in the soil solution may thus not only depend on soil pH, but also on the Ca^{2+} concentration (Römkens et al., 1996). By directly improving microbial growth conditions, i.e. improving nutrient availability and reducing pH-related toxicity, liming may reduce the metabolic costs of coping with adverse conditions and lead to an immediate increase in CUE in response to lime addition. Indirect effects on CUE may be caused by pH-related shifts in microbial communities (Soares and Rousk, 2019) which are strongly determined by soil pH (Lauber et al., 2008; Rousk et al., 2010a). With increasing soil pH, the fungal to bacterial ratio is likely to decrease (Rousk et al., 2010a). Given that the metabolisms of fungi may be less sensitive to stoichiometric constraints and nutrient availability as compared to bacteria (Keiblinger et al., 2010; Manzoni et al., 2012), this shift could decrease CUE. Besides liming effects on soil pH, liming may also affect CUE by Ca^{2+} addition. Recent results by Shabtai et al. (2023) showed that CUE increased in short-term response to Ca^{2+} addition, likely through the increase cation composition of mineral surface-layers, which promoted surface colonisation of metabolically efficient decomposers. Liming influences crop growth (Holland et al., 2019) and could indirectly affect CUE by changing quantity and quality of OC inputs (Mooshammer et al., 2014) with unknown consequences. In summary, it can be assumed that CUE is sensitive to the addition of lime and that the CUE is likely to increase.

Liming is a well-established management option for manipulating soil pH to an optimal range for plant nutrition (Truog, 1943). Liming is a practice in most agricultural soils, because fertilisation and extraction of cations results in soil acidification. In this study, we focus on the potential of liming to support the *in-vivo* pathway of SOC accrual as a side effect of liming. Liming of acidic soils was shown to increase SOC stocks, making it a potentially important management option for climate-change mitigation (Fornara et al., 2011; Wang et al., 2021). However, liming can have both positive and negative effects on C stocks (Paradelo et al., 2015) and the involved mechanisms remain elusive. In a review paper, Paradelo et al. (2015) outlined that the net effect of liming on SOC stocks is a result of stimulated microbial activity and thus decomposition (negative effect on SOC stocks), stabilisation of organic matter via formation of Ca^{2+} bridges and improved plant growth resulting in higher OC inputs (positive effects on SOC stocks) (Fig. 1). However, liming-induced changes in CUE may contribute to the net effect of liming on SOC stocks by altering the quantitative contribution of the *in-vivo* C stabilisation pathway. Most recently, Tao et al. (2023) posted that CUE may be the strongest predictor of SOC stocks at a global scale and common SOC models are highly sensitive to even small changes in CUE (Allison et al., 2010; Bölscher et al., 2020; Frey et al., 2013; Hyvönen et al., 1998). It can therefore be assumed that small changes in CUE could influence SOC stocks over extended periods of time. Thus, we expected that liming-induced changes in CUE at long-term field experiments translate in altered SOC stocks.

The first objective of this study was to investigate the response of CUE to liming-induced increases in soil pH across different initial pHs at agricultural field conditions. The second objective of this study was to test whether the observed long-term response of CUE would also occur immediately after the addition of lime in the laboratory. The third objective of this study was to evaluate C stocks changes with liming in conjunction with changes in microbial CUE, C_{mic}, and altered OC input to assess the potential benefit of modifying microbial CUE. Since C stocks build slowly, long-term field experiments were chosen for this study. Three available long-term liming experiments with initial soil pH at 4.5, 5.5 and 6.5 were selected for this study to cover the liming effect on the full pH range, i.e. liming from acidic - neutral, slightly acidic - alkaline). Control soils were additionally limed in the laboratory to test the immediate physiological response (within 1 week), and if the observed field-liming effect on CUE could be reproduced artificially. To assess whether shifts in microbial community composition were associated with changes in CUE, the abundances of microbial domains were quantified.

We hypothesised that i) long-term liming promotes higher microbial CUE, ii) that this effect is direct and related to amelioration of microbial growth conditions, and iii) that altered CUE translates into changes in SOC stocks.

2. Material and methods

2.1. Sites and sampling

2.1.1. Jyndevad 'P and liming' experiment

The long-term field experiment on liming and phosphorous (P) fertilisation in Store Jyndevad, Denmark (54°53′20″N 9°07′40″E; 16 m above sea level; MAT: 7.9 °C; MAP: 870 mm), was established in 1942–1944 (Azeez et al., 2020). The coarse-sandy soil (91.7 % sand, 4.1 % silt and 4.2 % clay) classifies as Haplic Podzol (IUSS Working Group WRB, 2015) developed from melt-water sand deposits and contains approximately 1.3 % C_{org} and 0.1 % N_{total} (measured in control soils in 2019). The experiment includes four P treatments combined with four liming treatments where lime is applied at rates of 0 Mg $CaCO_3$ ha^{-1} (*control*), 4 Mg $CaCO_3$ ha^{-1} (*lime 4*), 8 Mg $CaCO_3$ ha^{-1} (*lime 8*) and 12 Mg $CaCO_3$ ha^{-1} (*lime 12*) every 5–9 years in order to maintain target pH_{CaCl2} levels of 3.7, 5.4, 6.2 and 6.7, respectively (last limed in 2013). All treatments are performed in three replicates, with plots of 11.25 m × 8 m. Spring barley is cultivated every year since more than 35 years and nitrogen (N), potassium (K) and magnesium (Mg) are added at recommended rates. The field is ploughed to 20–22 cm every spring prior to seed bed preparation and crops are harvested in August always with removal of straw. All liming treatments of the high P plots (i.e. 156 kg P in 1944 + 15.6 kg P ha^{-1} $year^{-1}$) were included in this study, thus comprising 12 plots in total. Soil was sampled from 0 to 10 cm depth in October 2021 by pooling 6 soil cores (inner diameter 2 cm) from each plot. Samples were stored frozen until analysed. Measured soil pH ranged from pH_{H2O} 4.5–4.6 in the reference plots and from pH_{H2O} 5.6–7.3 in the limed plots.

2.1.2. Versailles '42 Parcelles' experiment

The Versailles '42 Parcelles' long-term bare-fallow experiment is an INRAE long term experiment located in the gardens of the Château de Versailles (48°48′12.8″N 2°05′09.9″E; 120 m above sea level; MAT: 10.7 °C; MAP: 628 mm), was established in 1928 to study the effect of long-term fertilisation as well as organic and basic amendments on physical soil properties of loamy soils (Barré et al., 2010; Burgevin and Hénin, 1939). The silty loam (17 % sand, 57 % silt and 26 % clay) classifies as Haplic Luvisol (IUSS Working Group WRB, 2015) developed in aeolian loess and contains 0.5 % C_{org} and 0.06 % N_{total} (measured in control soils in 2017). The experiment includes among other two lime treatments (CaO or $CaCO_3$ equivalent to 1 Mg CaO ha^{-1} y^{-1}), each in duplicate, and 10 control plots in total. All plots have a size of 2 m × 2.5 m and are kept free from vegetation by hand weeding and herbicide treatment and are manually ploughed twice a year to 25 cm depth (Barré et al., 2010). This study used archived samples of the four *limed* plots 26, 31, 39 and 40 (either with CaO or $CaCO_3$ amendment; last limed in 2016) and the *control* plots 22, 30, 32 and 34 (i.e. the nearest control plots to the limed plots) which were taken from 0 to 25 cm depth in 2017, 2-mm sieved and subsequently stored air-dried. Measured soil pH ranged from pH_{H2O} 5.2–6.0 in the reference plots, and from pH_{H20} 8.6–8.7 in the limed plots.

2.1.3. Dürnast 'Kalkversuch 016' experiment

The 'Dürnast Kalkversuch 016' field experiment was established in 1978 at Dürnast, Germany (48°24′16.82″ N, 11°42′04.52″ O; 464 m above sea level; MAT: 8.4 °C; MAP: 790 mm) classifies as Cambisol (IUSS Working Group WRB, 2015) developed from cover sand (Tucher et al., 2018). The loamy clay (48 % sand, 21 % silt and 31 % clay) contains 0.9 % C_{org} and 0.11 % N_{total} (measured in control soils in 2017). The experimental site includes three P treatments combined with three liming treatments (*control*, *Medium lime, High lime*). Lime is applied every 2–4 years (last limed in 2016 *Medium lime* and 2020 *High lime*) at a rate of 0.5–1.7 Mg CaO ha^{-1} (*Medium lime*) and 0.5–3.4 Mg CaO ha^{-1} (*High lime*) in order to maintain target pH_{CaCl2} of 6.2 and 6.7, respectively. All treatments are performed in four replicates, with plots of 8 m × 9.4 m. The crop rotation includes sugar beet, winter/spring wheat and winter/spring barley. Sulphur (S), N, K, and Mg are applied at levels adequate for plant growth. The site is managed ploughless since 2006. Crop residues (i.e. straw and sugar beet leaves) remain on the site. For this study, soil samples were taken from all liming treatments at the P application rate of 22 kg P ha^{-1} $year^{-1}$ in October 2021 (last crop: wheat) from a depth of 0–10 cm. Samples were stored frozen until analysed. Soil pH ranged from pH_{H2O} 6.3–6.7 in the reference plots and from pH_{H2O} 7.1–8.0 in the limed plots.

2.2. General soil parameters

Soil total organic C and N were determined on milled aliquots by dry combustion of 2 mm-sieved and 105 °C oven-dried soil samples. Additionally, samples with soil $pH_{H2O} > 6.5$ were analysed for carbonates via stepwise combustion at 450 °C for 12 h. Water holding capacity was quantified by soaking 10 g soil placed on a cotton wool-padded funnel with water. The water content quantified when water runoff stopped was assumed to represent 100 %WHC. Soil pH was measured in a 1:5 w/v ratio of soil to H_2O (1 h shaking horizontally, 200 rpm) using a FiveEasy pH meter with an LE438 electrode (Mettler-Toledo GmbH).

2.3. Determination of ^{18}O-CUE

Microbial CUE was determined by the ^{18}O-labelling method (Spohn et al., 2016) using the modifications previously described in Schroeder et al. (2021). Soils were pre-incubated at 15 °C for one week after adjusting the water content to 45 %WHC. Two aliquots of 300 mg soil were weighed into Eppendorf vials which were placed into 20 ml glass vials, and crimp-sealed. One aliquot was labelled by adding the exact amount of 80 at % enriched H_2–^{18}O to reach a label of 20 at %^{18}O in the final soil solution while adjusting water content to approximately 60 % WHC. The second aliquot received the same amount of unlabelled water and served as natural abundance reference. Shortly after adding the ^{18}O water (less than 1 min), the gas phase within the vial was evacuated and replaced with a standard gas at 350 ppm CO_2 (19.86 % O_2, 80.10 % N_2, 0.301 ppm N_2O, and 2.42 ppm CH_4) and 1300 mbar. Both labelled and unlabelled samples were incubated for 24 h at 15 °C. At the end of the incubation, a gas sample was taken from the labelled samples only by using a gas tight syringe. Subsequently, both vials were de-crimped. Soil samples were frozen in liquid nitrogen and stored at −80 °C until DNA extraction. Gas samples were analysed using a gas chromatograph equipped with an electron capture detector (Agilent 7890A GC, Agilent Technologies) and respiration flux ($C_{Respiration}$) was calculated from the increase in CO_2 concentration within 24 h incubation using the ideal gas equation according to Eq. (1):

$$C_{Respiration}\left[\text{ng C g}^{-1}\text{soil h}^{-1}\right] = \frac{p \times V}{R \times T} \times M \times \Delta CO_2 \times \frac{1}{\text{g soil} \times 24\text{ h}} \quad \text{Eq.1}$$

where p is the pressure [kPa] in the vial (1300 kPa), V is the volume [l] of the vial headspace, R is the universal gas constant (8.314 L kPa K^{-1} mol^{-1}), T is the temperature [K] at which the standard gas is injected into the vial (293 K), M is the molecular mass of carbon (12.01 g mol^{-1}), and ΔCO_2 is the increase in CO_2 concentration [ppm] during the incubation time of 24 h [h].

DNA was extracted using the FastDNA™ SPIN Kit for Soil (MP Biomedicals) following the standard protocol, with an extension of the centrifugation to 15 min in step five (15.000 rpm, Sigma 4-16 KS). The DNA concentration in the extracts was quantified with the QuantiT PicoGreen dsDNA Kit (Invitrogen). The isotopic signatures of dried DNA extracts (oven-dried at 60 °C in silver capsules) were measured using a high-temperature conversion/elemental analyser (TC/EA) (Thermo Fisher Scientific) coupled with a Delta V Plus isotope ratio mass spectrometer via a ConFloIV interface (Thermo Fisher Scientific).Microbial growth rate (C_{Growth}) was calculated based on the incorporation of ^{18}O from the labelled soil solution into the microbial DNA based on the enrichment, the average proportion of oxygen in DNA and a sample specific conversion factor from DNA to C_{mic}, i.e. *fDNA* according to Eq. (2):

$$C_{Growth}\left[\text{ng C } g^{-1}\ soil\ h^{-1}\right] = DNA\ O\ \left[\mu g\right] \times \frac{DNA\ ^{18}O\ \left[\text{at\%excess}\right]}{enrichment\ \left[\text{at\% }^{18}\text{O}\right]} \times \frac{100}{31.21\ \left[\%w/w\right]} \times fDNA \times \frac{1}{g\ soil \times 24\ h} \quad \text{Eq.2}$$

where *DNA O* [µg] is the total amount of O in the DNA eluate derived from the isotopic analysis, *DNA ^{18}O* [at% excess] is the difference in at % ^{18}O between the labelled and the unlabelled natural abundance control samples, and the *enrichment* of the final soil solution is adjusted to 20 at % ^{18}O. The average % w/w of O in DNA is 31.21 ($C_{39}H_{44}O_{24}N_{14}P_4$).

To be able to calculate the conversion factor *fDNA*, C_{mic} was determined after pre-incubation by the chloroform fumigation extraction (CFE) method (Vance et al., 1987). In brief, fumigation was conducted for 24 h at room temperature in the dark, using an excess amount of chloroform ($CHCl_3$). The non-fumigated and fumigated 5 g soil aliquots were extracted with 0.5 M K_2SO_4 in a 1:4 soil-to-extractant ratio (30 min horizontal shaking at 200 rpm) and filtered. Non-purgeable organic carbon (NPOC) was analysed in a 1:4 v/v extract dilution after removal of total inorganic C by adding 15 % HCl in order to adjust to pH 2–3 and outgassing emerging CO_2 for 5 min with artificial air (Dimatoc 2000; DIMATEC Analysetechnik). Microbial biomass C was calculated with a conversion factor (k_{EC}) of 0.45 (Joergensen, 1996).

The microbial CUE (Eq. (3)) is defined as microbial biomass C produced (C_{Growth}) over the total uptake of C, approximated as the sum of microbial biomass C produced and C respired ($C_{Respiration}$) (Manzoni et al., 2012):

$$CUE = \frac{C_{Growth}}{C_{Growth} + C_{Respiration}} \quad \text{Eq.3}$$

2.4. Estimating microbial abundance by qPCR

The abundances of bacteria, archaea and fungi were estimated from the non-labelled DNA extracts by qPCR using the CFX96 Touch™ Real-Time PCR Detection System (Bio-Rad Laboratories) (Hemkemeyer et al., 2015). The abundance of archaea and bacteria was estimated according to the TaqMan probe approach. Amplification of the 16S rRNA gene of archaea and bacteria was conducted using the primers ARC787F, ARC1059R, and BAC338F, BAC805R, respectively. The probes ARC915F and BAC516F were used for quantification of the same gene (Yu et al., 2005). Fungal ITS1 sequences were amplified using the primers NS1 and 58A2R and quantified by SYBR Green (Martin and Rygiewicz, 2005). Reactions were carried out in duplicates from 50 × and 100 × dilutions of the DNA extracts. DNA templates from pure cultures of *Bacillus subtilis*, *Methanobacterium oryzae* and *Fusarium culmorum* were used to generate standard curves. The PCR efficiencies were 95.3 ± 1.2 % SD ($R^2 = 0.998$) for archaea, 87.7 ± 1.2 % SD ($R^2 = 0.997$) for bacteria, and 98.9 ± 4.0 % SD ($R^2 = 0.995$) for fungi.

2.5. Laboratory liming experiment

An additional experiment was conducted to examine the immediate response of CUE to laboratory liming (hereafter lab liming) using control soils of all three long-term field experiments, where soil pH was raised to a level equivalent to that of field-liming treatments. The amount of lime that needed to be added to the control soils was determined in a preliminary test. In the pre-experiment, $CaCO_3$ (95 % $CaCO_3$ 95, DüKa Düngekalkgesellschaft GmbH) was added at a rate of 25 %, 50 % and 125 % of the field application rate. Soil pH_{H2O} was determined in a 1:5 soil-to-water dilution after pre-incubating the limed soils for 1 week at 15 °C and a water content in the range between 45 %WHC and 60 % WHC. The specific amount of $CaCO_3$ to reach the targeted soil pH was then derived from the linear increase in soil pH with lime in the pre-experiment. For the laboratory-liming experiment the specified amount of $CaCO_3$ was added, water content adjusted to range between 45 %WHC and 60 %WHC and samples pre-incubated for 1 week at 15 °C before ^{18}O-CUE measurement according to the protocol. Laboratory liming adjusted soil pH closest to the treatments *lime 8* at Jyndevad and *Medium lime* at Dürnast. Yet, laboratory liming did not adjust the soil pH to the exact level as in *limed* plots at Versailles, but successfully shifted the soil pH from acidic to neutral.

2.6. Differentiation between microbial respiration and lime-derived CO_2 emissions using $\delta^{13}C$ signatures

The addition of lime to the soils causes a shift of the chemical equilibrium to the dissociation site (Eq. (4)). Thereby, soil acidity is neutralised and CO_2 evolves from the soil:

$$CaCO_3 + 2\,H^+ \rightleftharpoons Ca^{2+} + CO_2 + H_2O \quad \text{Eq.4}$$

It was shown that lime-derived CO_2 emissions were detectable in the field during the first 2–4 months after lime application and lime-derived CO_2 made up for more than 50 % of the CO_2 emission in a short-term laboratory incubation (Biasi et al., 2008). To accurately determine microbial respiration for CUE assessment it is therefore necessary to separate abiotic and biotic CO_2 production, i.e. respiration-derived and lime-derived CO_2 emissions. Therefore, we determined the $\delta^{13}C$ signatures of gas samples relative to the Vienna-Pee Dee belemnite (V-PDB). The relative proportions of both fractions were calculated using a two-pool isotope mixing model (Bertrand et al., 2007; Biasi et al., 2008). Gas samples taken after 24 h of incubation were analysed for their $\delta^{13}C$ signatures using a Delta plus XP via a Conflo III interface (Thermo Fisher Scientific, Bremen, Germany). The $\delta^{13}C$ signatures of gas samples were blank-corrected using a Keeling plot with two points in order to assess the $\delta^{13}C$ signatures of the CO_2 emission from the soil. The $\delta^{13}C$ signature of the lime was -1.67 ± 0.11‰ SD and was determined in five replicates using an Elemental Analyzer (EA) Flash 2000 coupled with a Delta V IRMS via a ConFlo IV interface (Thermo Fisher Scientific, Bremen, Germany).

The contribution of lime-derived CO_2 to total CO_2 emissions could only be assessed for the laboratory liming experiment and was calculated following the two-pool mixing model:

$$\%\ lime\ derived\ CO_2 = \frac{\left(\delta^{13}C_{limed} - \delta^{13}C_{control}\right)}{\left(\delta^{13}C_{lime} - \delta^{13}C_{control}\right)} \times 100 \quad \text{Eq.5}$$

Where δ_{limed}, $\delta_{control}$, and δ_{lime} are the isotopic signature of the CO_2 emissions for limed samples, non-limed control samples, the added lime, respectively. The model applies under the assumption that an isotopic equilibrium between lime-carbonates and lime-derived CO_2 exists and that the dissolution of $CaCO_3$ and subsequent formation of CO_2 does not cause isotope fractionation.

Lime-corrected CUE values were calculated according to Eq. (6), where the microbial respiration ($C_{Respiration}$) rate was calculated as the remaining percentage of the CO_2 evolving from soil (*CO_2 emission rate* in ng C g^{-1} soil h^{-1}) after lime-derived CO_2 emissions (*% lime derived CO_2*) were subtracted.

$$CUE_{lime\ corrected} = \frac{C_{Growth}}{C_{Growth} + \left(\left(1 - \frac{\%\ lime\ derived\ CO_2}{100}\right) \times CO_2\ emission\ rate\right)} \quad \text{Eq.6}$$

Indeed, CO_2 emissions from limed soils were increased as compared to non-limed control soils during the 24h of incubation, although soils were pre-incubated for one week subsequent to laboratory lime addition (Fig. 2). An average of 69 ± 4 % SD (Jyndevad), 57 ± 2 % SD (Versailles) and 22 ± 3 % SD (Dürnast) of the CO_2–C evolving from the soil originated from the lime. According to the $LME_{overall}$, lime-corrected $C_{Respiration}$ was only affected at Jyndevad, where it doubled in response to lab liming ($p_{adj} < 0.001$) (Table S1).

2.7. Calculation of soil organic C stocks and organic C inputs

To investigate whether liming stimulates SOC accrual in long-term, we calculated cumulative SOC stocks. Cumulative SOC stocks [Mg C ha^{-1}] for the topsoil were calculated using Eq. (7), where *SOC* is the total organic carbon content [%], *BD* is the bulk density of fine earth excluding rock fragments calculated as mass of fine earth over total sample volume [g cm^{-3}], and *depth* is the thickness of the sampled topsoil layer [cm].

$$SOC\ stock\ \left[Mg\ C\ ha^{-1}\right] = \frac{SOC}{100} \times BD \times depth \times 100 \quad \text{Eq.7}$$

Bulk density differed significantly between treatments at Versailles, with the lowest mean treatment bulk density in limed plots (Paradelo et al., 2016). At Dürnast, bulk density did not differ between treatments as tested using a linear mixed-effects model approach. For valid comparison, SOC stocks were thus calculated based on the mean bulk density of the limed soils at Versailles (1.25 Mg m^{-3}), and based on mean bulk density at Dürnast (1.15 Mg m^{-3}) and Jyndevad (1.37 Mg m^{-3}, reported by Azeez et al., 2020). The change in SOC stock with liming was expressed as Δ SOC stock [Mg C ha^{-1}] and calculated as difference between the mean SOC stocks of the respective limed treatment and the control soil.

Organic C inputs were calculated from available long-term experimental yield and management data based on C_{org} allocation factors according to Jacobs et al. (2020), and averaged over all years as mean annual OC input (Mg C ha^{-1} $year^{-1}$). It was taken into account that at Dürnast the straw remained on the field, while at Jyndevad it was removed. There were no additional inputs from cover crops or organic fertilisation at either site. The change in OC input with liming (Δ OC input) was calculated as difference between the mean OC input of the respective limed treatment and the control soil. Cumulative Δ OC input was calculated for the time since the experiment was running until sampling (i.e. Jyndevad: 77 years, Dürnast: 43 years). SOC formation efficiency was then calculated as ratio between Δ SOC stock and cumulative Δ OC input.

2.8. Statistics

Statistical analyses and data visualisation were conducted in R v4.1.2 (2021-11-01) (R Core Team, 2020) using RStudio v2022.12.0 (Posit team, 2022). The following packages were used: *tidyverse* (Wickham et al., 2019), *RcolorBrewer* (Neuwirth, 2014), *lme4* (Bates et al., 2015), *lmerTest* (Kuznetsova et al., 2017), *emmeans* (Lenth 2021), *multcomp* (Hothorn et al., 2008), *multcompView* (Graves et al., 2019), *ggpmisc* (Aphalo, 2021), *hrbrthemes* (Rudis, 2020) and *cowplot* (Wilke, 2020). Unless otherwise stated, the values below are given as mean ± standard deviation. Data and R code used for this study are freely available at [10.5281/zenodo.10137003].

Different linear mixed-effects model (LME) approaches were used to

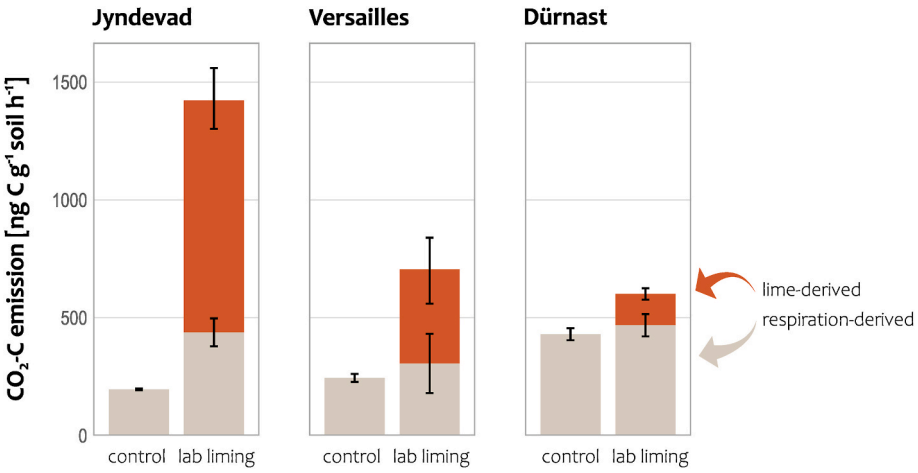

Fig. 2. Mean absolute CO_2–C emissions ± standard deviation from the control soils per site, incubated without (i.e. control) and after laboratory addition of lime (i.e. lab liming). The colours indicate the source of CO_2–C emissions as differentiated based on the $\delta^{13}C$ signatures (orange: lime-derived, grey: respiration-derived).

test i) if long-term field liming and laboratory liming have a general effect on soil pH and microbial parameters ($LME_{overall}$), and ii) if there are site-specific treatment effects on the before mentioned parameters, allowing to identify which liming level, (i.e. treatment) causes significant changes ($LME_{site\text{-}wise}$). $LME_{overall}$ included *site* and *liming* (levels: control, field liming, lab liming) as fixed effects. *Block* was included as random effect (random intercept) to consider the field-design. An additional random effect (random intercept) for the *parcel* from which the soil was sampled was introduced into the LME to account for the dependence between the control soils and the corresponding laboratory limed samples. Due to the different number of field treatments between sites it was necessary to subset the data for the $LME_{overall}$ in order to keep the statistical design balanced, and the field treatment with soil pH being closest to the laboratory limed soils according to Table 1 was selected (Jyndevad: *lime 8*; Versailles: *limed*; Dürnast: *Medium lime*). This choice allowed us to compare the effects of direct and long-term lime addition on microbial parameters, while excluding differences in the magnitude of the pH shift. The $LME_{overall}$ was also used to assess significant differences between sites. In addition, we tested for an interactive effect between *site* and *liming* by implementation of two models: one allowing for their interaction and thus that the effect of liming differs across sites and another one without this interaction. The model with the lowest Akaike Information Criterion (AIC) was considered for the $LME_{overall}$ analysis. If not indicated differently, the model allowing for the interaction was implemented. $LME_{site\text{-}wise}$ was used to test for differences between treatments at individual sites. The model included *treatment* as fixed effect and *block* and *parcel* as random effects (random intercepts). For all LME a visual inspection of residual plots was used to check for deviations from homoscedasticity or normality, and data was log-transformed where necessary. Significance of the fixed effect was assessed at a significance level of $\alpha = 0.05$. Estimated marginal means were calculated and differences between treatments are given as a compact letter display in the respective tables at a significance level of $\alpha = 0.05$. In addition, liming-induced shifts compared to the control are either indicated as 95 % confidence intervals of the estimated difference to the control ($\Delta_{estimate}$) or given as estimated mean response ratio ($RR_{estimate}$) and were specifically tested based on LME estimated marginal means by setting contrasts for treatments to the control. The p-values and confidence intervals were adjusted according to Sidak for multiple comparison correction.

We hypothesised that liming altered microbial parameters through the shift in soil pH, and therefore assumed a relationship between microbial parameter and soil pH over the different levels of long-term liming intensity, i.e. treatments. This correlation was assumed if the Pearson coefficient of correlation between microbial parameter and soil pH had a p-value of $p < 0.05$ for site-wise linear regression. To describe the general relationship between soil pH and microbial parameters (CUE, C_{Growth}, $C_{Respiration}$, C_{mic}) measured values were z-transformed. This allowed to perform a regression over the combined data set (only considering field-limed treatments). Linear, exponential, log and polynomial regressions (e.g. quadratic) were tested and the best fit chosen by the lowest AIC value.

To link potential liming-induced shifts in microbial physiology to C cycling, we investigated effects of long-term liming on SOC stocks (all sites included) and OC inputs (Jyndevad and Dürnast). We tested for a general effect of liming on C stocks using a modified $LME_{overall}$ (fixed: *liming* and *site*, random: *block*) on a subset of data including only control plots and the highest liming level treatment of each site, in order to keep the statistical design balanced. Site-specific treatment effects on C stocks were tested using a modified $LME_{site\text{-}wise}$ at Dürnast and Jyndevad (fixed: *treatment*, random: *block*), while for Versailles in the absence of the grouping *block* factor, we applied an ANOVA with *treatment* as independent variable and *C stocks* as dependent variable ($\alpha = 0.05$). To test whether long-term liming increases OC inputs we used another site-wise LME approach (LME_{input}) with *liming* and *main crop* as fixed effects, allowing for their interaction and thus, that the effect of liming on OC inputs differs depending on the main crop. Site was not included as fixed effect in LME_{input}, since no main crop was replicated across different

Table 1
Treatment effects on soil pH at individual sites. Soil pH per treatment is given as measured mean ± standard deviation. Differences were tested using site-wise linear mixed-effects modelling. Significant differences in soil pH were found between treatments displaying different letters (per site). The difference in soil pH to the control treatment (ΔpH) is indicated as lower and upper boundary of the 95 % confidence interval of the estimated marginal mean difference. Confidence intervals and p-values (p_{adj}) were adjusted according to Sidak to correct for multiple comparisons of treatments to the control.

Site	Treatment	pH_{H2O}				ΔpH (95 %CI)			p_{adj}
Jyndevad	control	4.5	±	0.1	d				
	lime 4	5.7	±	0.1	c	0.9	–	1.4	**< 0.001**
	lime 8	6.9	±	0.2	b	2.1	–	2.6	**< 0.001**
	lime 12	7.3	±	0.1	a	2.5	–	3.0	**< 0.001**
	lab liming	6.7	±	0.1	b	1.7	–	2.6	**< 0.001**
Versailles	control	5.5	±	0.3	c				
	limed	8.6	±	0.0	a	2.7	–	3.5	**< 0.001**
	lab liming	7.2	±	0.2	b	1.3	–	2.0	**< 0.001**
Dürnast	control	6.5	±	0.2	c				
	Medium lime	7.4	±	0.2	b	0.5	–	1.2	**< 0.001**
	High lime	7.8	±	0.1	a	1.0	–	1.7	**< 0.001**
	lab liming	7.4	±	0.1	b	0.6	–	1.1	**< 0.001**

sites. *Year, parcel*, i.e. specific sample plot at a given site, and *block* were introduced as random effects (random intercepts).

3. Results

3.1. Effects of liming on microbial CUE

While liming increased soil pH by 0.5–3.0 pH units depending on the liming intensity (Table 1), we found that long-term liming changed CUE in opposite directions, i.e., leading to increased or reduced CUE depending on the initial soil pH: Increasing soil pH_{H2O} from 4.5 to 7.3 resulted in a significant decline by 40 % in microbial CUE from 0.46 ± 0.07 in control soils to 0.28 ± 0.03 in highest limed plots (Jyndevad). At Versailles, the increase in soil pH_{H2O} to alkaline conditions from 5.5 to 8.6 (Versailles) increased CUE by 16 %, i.e. from 0.73 ± 0.11 to 0.85 ± 0.05 in limed plots. The shift from pH_{H2O} 6.5 to 7.8 (Dürnast) was associated with a significant increase in microbial CUE of 24 %, i.e. from 0.34 ± 0.03 in control soils to 0.42 ± 0.02 at highest field-liming level. Hence, there was no generalisable effect of liming on CUE across all sites as revealed by a non-significant fixed *liming* effect in the $LME_{overall}$ (Table 2). CUE differed significantly between sites ($p = 0.0033$) and the model confirmed that liming had opposing effects on CUE depending on site, as shown by a significant interaction effect between *liming* and *site* ($p < 0.001$) (Table 2). The responses of CUE to field and lab liming pointed in the same direction. According to the $LME_{overall}$, field and lab liming significantly reduced CUE at Jyndevad, whereas both liming applications increased microbial CUE as compared to the control at Versailles. At Dürnast, no effect of *Medium lime* addition or *lab liming* was detected in the $LME_{overall}$. However, using the $LME_{site\text{-}wise}$ considering all field-liming treatments, we found the CUE of highest-level field-liming treatments to differ significantly from control soils at Jyndevad ($p_{adj} = 0.0489$) and Dürnast ($p_{adj} = 0.0052$), with opposing estimated effects, i.e. negative at Jyndevad and positive at Dürnast (Table S2). Using $LME_{site\text{-}wise}$ no differences were found between treatments at Versailles, which is likely related to the variation in the data and the smaller power of the $LME_{site\text{-}wise}$ approach. In line with the results of the LMEs, the linear regression showed that shifts in soil pH with long-term liming affected microbial CUE with opposing trends for the investigated sites (Fig. 3A): CUE was negatively correlated to soil pH at Jyndevad ($p = 0.008$), not significantly affected at Versailles but tended to increase with higher soil pH, and positively correlated to soil pH at Dürnast ($p = 0.016$). Site-wise linear regression did not indicate any correlation between the lime-induced shift in soil pH and CUE for lab-limed soils, but trends in CUE with lab liming pointed into the same direction as with long-term liming (Fig. 3A). Since the range of CUE values differed between sites, microbial CUE data (*lab liming* excluded) was normalised by site-wise z-transformation to investigate the general pattern of the relationship between microbial CUE and soil pH (Fig. 3B). The pH-dependency of microbial CUE was best described by a quadratic fit and followed a U-shaped curve with lowest microbial CUE at near neutral soil $pH_{H2O} = 6.4$, where soil pH explained 36 % of the variation in z-transformed CUE.

3.2. Effects of liming on microbial biomass C, microbial growth and respiration

Liming increased C_{mic} at all sites ($p = 0.0088$) without significant interaction of *site* and *liming* according to the $LME_{overall}$. At individual sites, increases in C_{mic} with liming were however only significant for *High lime* and *lab liming* treatments at Dürnast according to the $LME_{site\text{-}wise}$ (Table S2). C_{mic} increased linear with soil pH, both at individual sites (Fig. 4A) and across sites (Fig. 4B). The proportion of microbial biomass C to SOC, i.e., C_{mic}/C_{org} was significantly increased at Jyndevad with liming ($LME_{site\text{-}wise}$, *lime 12* $p_{adj} = 0.00178$), non-significantly affected at Versailles, and tended to increase at Dürnast ($LME_{site\text{-}wise}$, *High lime* $p_{adj} = 0.0677$) (Table 3). Overall, *lab liming* significantly increased K_2SO_4-extractable C by 36 % as compared to control treatments, while *field liming* showed 28 % lower values as controls ($LME_{overall}$ $p < 0.05$) (Table S3). This was however non-significant if considered individual sites using $LME_{site\text{-}wise}$ (Fig. S1).

To focus on the effects of liming on microbial physiology, we excluded the effects of liming on microbial respiration and growth which were related to the increase in microbial biomass by normalising $C_{Respiration}$ and C_{Growth} by C_{mic} to represent mass specific activity rates (Fig. 5). While total $C_{Respiration}$ increased with liming ($p < 0.001$), we found that specific $C_{Respiration}$ (aka metabolic quotient) was not significantly affected by lime addition according to the $LME_{overall}$ (Fig. 5, Table S1). This indicates microbial respiration increased proportionally with microbial biomass in response to liming. In contrast, specific C_{Growth} was significantly affected, with the response to liming depending on the site as seen by a significant interaction effect of *liming* and *site* in the $LME_{overall}$ ($p < 0.001$). Specific C_{Growth} was reduced with the long-term liming-induced shift towards neutral pH at Jyndevad (Fig. 5B), and was unaltered at Versailles and Dürnast. Only at Versailles, *lab liming* significantly stimulated specific C_{Growth} according to the $LME_{overall}$ ($p_{adj} = 0.0052$).

The relationship between specific $C_{Respiration}$ and specific C_{Growth} with soil pH was less pronounced than the relationship between CUE and soil pH. And site-wise linear regression only revealed a significant correlation between specific C_{Growth} and soil pH at Jyndevad ($p < 0.001$; $R^2_{adj} = 0.855$). Interestingly, the general pattern of z-transformed $C_{Respiration}$ and C_{Growth} showed opposing optimum curves (Fig. S2). The pattern of the relationship between $C_{Respiration}$ and soil pH was best described by a second-grade polynomial-fit following an upside-down U-

Table 2
Overall effects of field and laboratory liming (i.e. lab liming) on microbial carbon use efficiency (CUE). Effects of liming on microbial CUE were tested using a linear mixed-effects model approach across all sites ($LME_{overall}$). The model was run on a subset dataset including only the field liming treatment with the soil pH closest to lab liming to allow direct comparison. Significant differences between treatments at each site are indicated by different grouping letters. The effect of respective liming is indicated as estimated response ratio of the treatment to the control ($RR_{estimate}$) together with the respective Sidak adjusted p-values (p_{adj}). Treatments in bold differed significantly from the control. Significance of the fixed effects is indicated by p-value at a level of significance $\alpha = 0.05$.

$LME_{overall}$	CUE ~ Site * Liming + (1 | block) + (1 | parcel)						
Site	Liming	group	$RR_{estimate}$	p_{adj}	Fixed effects		p-value
Jyndevad	control	a			**Site**	**	**0.0033**
	field liming (lime 8)	b	**0.69**	**<0.001**	Liming		0.5419
	lab liming	b	**0.84**	**0.0299**	**Site:Liming**	***	**<0.001**
Versailles	control	b					
	field liming (limed)	ab	**1.18**	**0.0441**			
	lab liming	a	**1.16**	**0.0324**			
Dürnast	control	a					
	field liming (Medium lime)	a	1.07	0.5128			
	lab liming	a	0.97	0.7421			

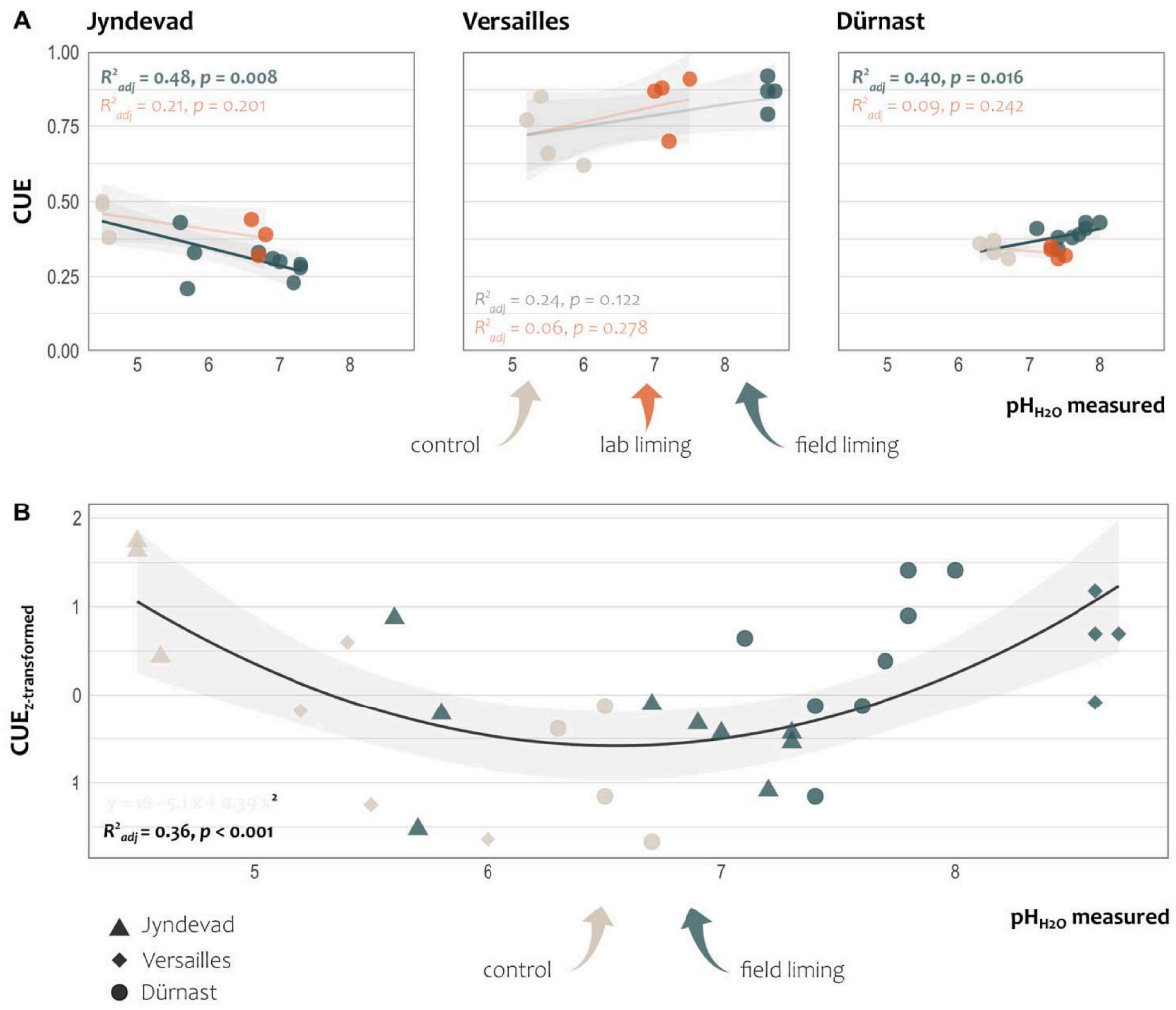

Fig. 3. Microbial carbon use efficiency (CUE) is linked to the liming-induced shift in soil pH. **A)** Absolute CUE values for control soils (grey), field liming (green) and lab liming (orange) are given per site. Liming was considered to have a significant effect on CUE due to changes in soil pH if the linear regression indicated a relationship with soil pH at $p < 0.05$. **B)** Data was z-transformed (based on mean and standard deviation per site) to reduce site-dependent differences in CUE (lab liming not included). This allowed to investigate the general relationship between CUE and soil pH, which was found to describe a U-curve (quadratic fit; $p < 0.05$).

shape ($p = 0.039$), while the best fit for C_{Growth} indicated a U-shaped relationship ($p = 0.016$), indicating the highest respiration with lowest growth rate at near neutral soil pH. Soil pH was only explaining 14.5 % and 19.5 % of the variance in the z-transformed $C_{Respiration}$ and C_{Growth}, respectively. However, the combined patterns result in a much stronger relationship between CUE and soil pH as described above.

3.3. Effects of liming on abundance of microbial domains

The estimated abundances of bacteria and archaea by their 16S rRNA gene copies differed significantly between sites ($LME_{overall}$ $p < 0.001$). At Jyndevad, all long-term liming treatments resulted in significantly increased bacterial abundance as compared to control, whereas treatment effects on bacterial abundance were non-significant for Versailles and Dürnast (Fig. 6). In line with the $LME_{site\text{-}wise}$, we found a significant positive correlation between bacterial abundance and soil pH at Jyndevad, but not for the two other sites (Fig. 6A). Archaeal abundance was affected by liming with the effect differing between sites, according to a significant interaction effect in the $LME_{overall}$ ($p = 0.0071$). The abundance of archaea was significantly higher in long-term limed soils at the Versailles bare fallow experiment ($LME_{overall}$ $p_{adj} < 0.001$), which was also supported by a significant positive correlation between archaeal abundance and soil pH at that site (Fig. 6B). Effects of site and liming on fungal abundance, as estimated by ITS1 copy numbers, were not significant according to the $LME_{overall}$. At Versailles, fungal abundance was significantly reduced in long-term limed soils as compared to the control soils, only if specifically tested by setting contrast for field liming to the control in the $LME_{site\text{-}wise}$ ($p_{adj} = 0.0356$). However, as seen from the significant correlations between fungal abundance and soil pH, the shift in soil pH from initially acidic conditions at Jyndevad ($pH_{H2O} = 4.5$) and Versailles ($pH_{H2O} = 5.5$) towards neutral pH reduced fungal abundance. Yet, fungal abundance was not significantly altered by long-term liming in Dürnast, where the initial pH was already neutral. In contrast to long-term liming, *lab liming* did not alter estimated abundances of fungi, bacteria and archaea at any of the sites (Table S2, Fig. 6).

3.4. Effects of long-term liming on SOC stocks and OC inputs

Overall, long-term liming had a significant positive effect on SOC stocks ($LME_{overall}$ $p = 0.0032$). Using $LME_{sitewise}$ to assess treatment differences, limed soils showed significantly higher SOC stocks than control soils only at Versailles ($p_{adj} = 0.0155$) (Table S4), with 22 ± 3 Mg C ha^{-1} in limed plots as compared to 17 ± 2 Mg C ha^{-1} in control plots. No significant differences were found in SOC stocks between limed and control soils at Jyndevad and Dürnast, but SOC stocks tended to increase with liming. Consistently, Versailles was the only site showing a significant positive correlation between SOC stocks and soil pH, with soil

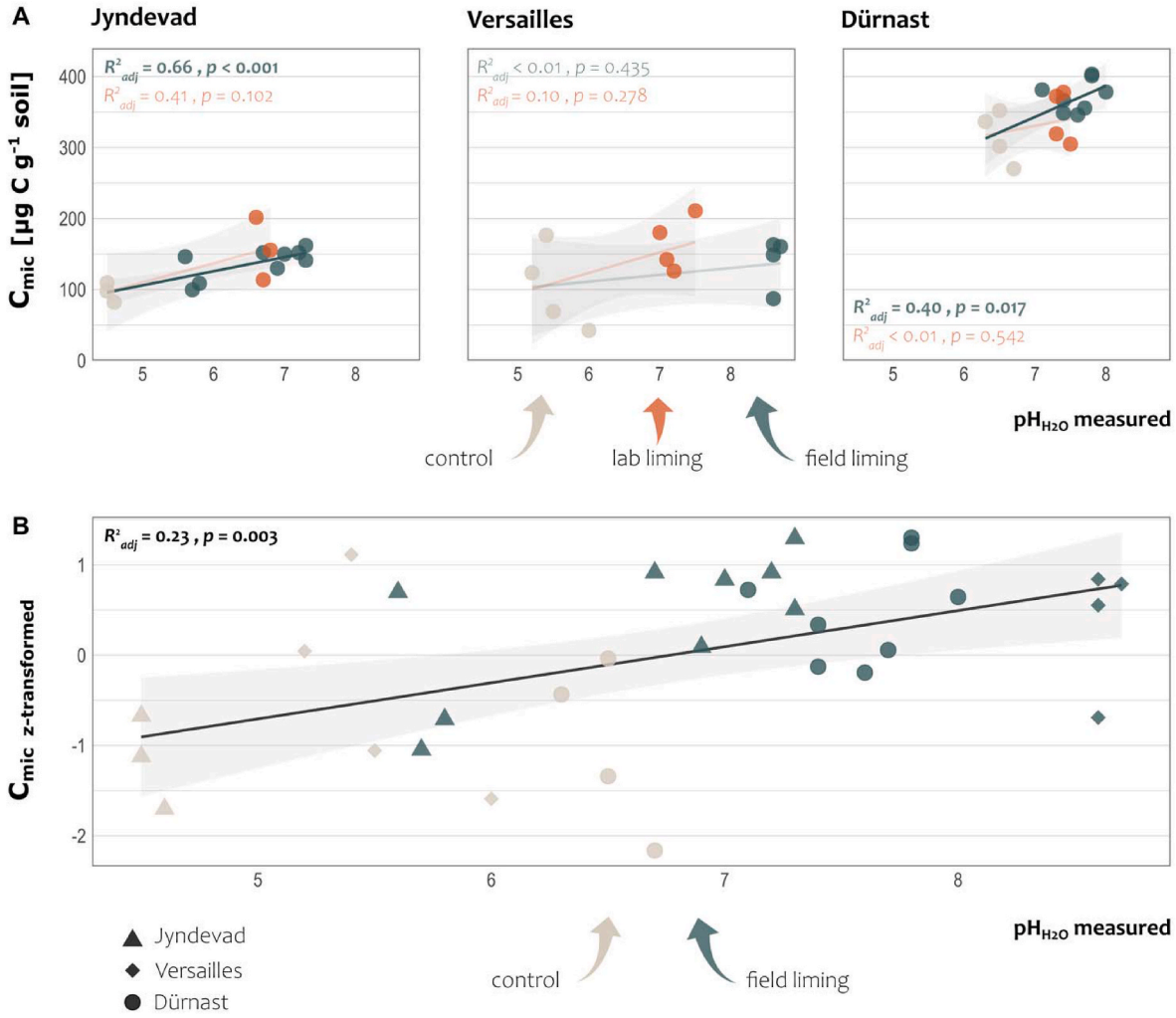

Fig. 4. Microbial biomass C (C_{mic}) increased with the liming-induced shift in soil pH. **A)** Absolute C_{mic} values for control soils (grey), field liming (green) and lab liming (orange) are given per site. Liming was considered to have a significant effect on C_{mic} due to changes in soil pH if the linear regression indicated a relationship with soil pH at $p < 0.05$. **B)** Data was z-transformed (based on mean and standard deviation per site) to reduce site-dependent differences in C_{mic} (lab liming not included). This allowed to investigate the general relationship between C_{mic} and soil pH, which followed a linear relationship ($p < 0.05$).

Table 3
Site-wise long-term liming effects on the relative proportion of microbial biomass (C_{mic}) to soil organic C (C_{org}) (%). Values are given as the measured mean ± standard deviation. C_{mic}/C_{org} differed significantly between treatments marked with different letters. The estimated marginal mean differences of treated soils to the control treatment ($\Delta_{estimate}$) are indicated as lower and upper boundary of the 95 % confidence interval (CI). The confidence intervals and p-values (p_{adj}) were calculated by setting contrasts of treatments to the control and adjusted according to Sidak to correct for multiple comparisons. Treatments differing significantly from control are indicated by bold p_{adj} ($\alpha = 0.05$).

$LME_{site\text{-}wise}$		C_{mic}/C_{org}							
Site	Treatment	mean ± sd				$\Delta_{estimate}$ (95 %CI)			p_{adj}
Jyndevad	control	0.76	±	0.13	b				
	lime 4	0.94	±	0.16	ab	−0.12	–	0.48	0.2619
	lime 8	1.09	±	0.08	ab	**0.03**	-	**0.63**	**0.0320**
	lime 12	1.14	±	0.09	a	**0.08**	-	**0.67**	**0.0178**
Versailles	control	1.95	±	1.27	a				
	limed	2.04	±	0.67	a	−1.67	–	1.85	0.9060
Dürnast	control	3.35	±	0.27	a				
	Medium lime	3.69	±	0.31	a	−0.25	–	0.94	0.2606
	High lime	3.90	±	0.28	a	−0.05	–	1.15	0.0677

pH explaining 55 % of the variation in SOC stocks (Fig. 7). Observed changes in microbial CUE with long-term liming were not correlated to SOC stocks for each individual site.

At the two sites of Jyndevad and Dürnast, OC inputs increased significantly with liming (Fig. S3, Table S5). At Jnydevad Δ OC input of 1.03 Mg C ha^{-1} yr^{-1} (*lime 4*), 1.25 Mg C ha^{-1} yr^{-1} (*lime 8*), and 1.14 Mg C ha^{-1} yr^{-1} (*lime 12*) ($p_{adj} < 0.001$). In comparison, changes in OC inputs with liming were smaller at Dürnast, where OC input increased by

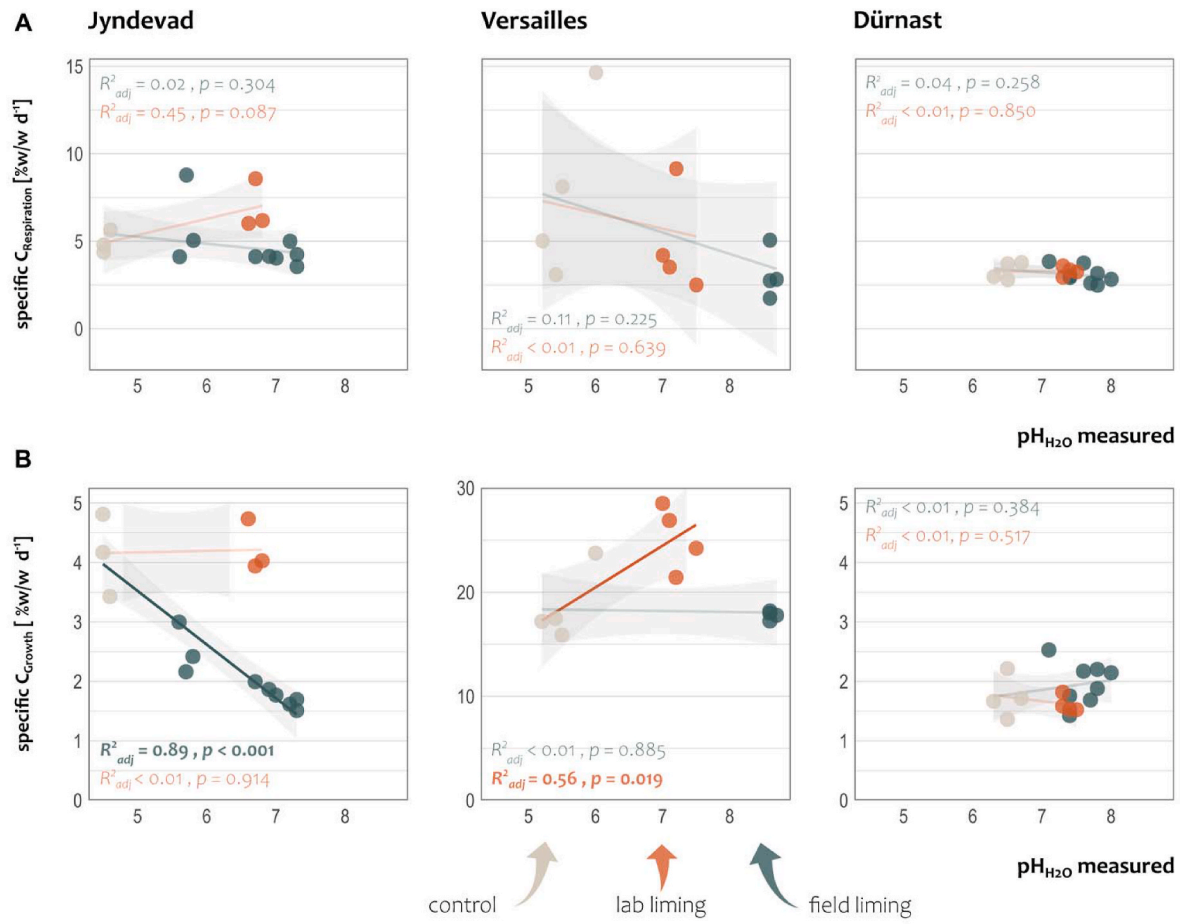

Fig. 5. Mass specific microbial respiration and growth rates, i.e. the relative proportion of C as compared to the standing microbial biomass C which is directed to microbial respiration or growth per day. **A)** Specific microbial respiration was not significantly affected by the shift in soil pH with liming, whereas **B)** specific microbial growth rate was reduced significantly with long-term liming at Jyndevad and increased with lab liming at Versailles. Colours indicate control soils (grey), field liming (green) and lab liming (orange). Long-term liming was considered to have a significant effect if the linear regression indicated a relationship with soil pH at $p < 0.05$. Please note different y-axis scales in B).

0.344 Mg C ha^{-1} yr^{-1} for *Medium lime* (p_{adj} = 0.036) and 0.180 Mg C ha^{-1} yr^{-1} for *High lime* (ns).

SOC formation efficiency was 9.6 % (*Medium lime*) and 21.4 % (*High lime*) at Dürnast, and −0.6 % (*lime 4*), 1.3 % (*lime 8*), and 2.1 % (*lime 12*) at Jyndevad. The SOC formation efficiency of OC inputs was thus much lower in Jyndevad as compared to Dürnast.

4. Discussion

4.1. The liming response of CUE depends on the pH range

The general relationship between CUE and soil pH followed a U-shaped curve (i.e. quadratic), with lowest CUE at pH$_{H2O}$ = 6.4. Whether liming increased or reduced CUE was site-specific (i.e. interaction effect of site and liming), and depended on the initial soil pH. At Jyndevad and Dürnast, CUE was linearly correlated to soil pH across increasing liming intensities, explaining 48 % and 40 % of variation in CUE, respectively (Fig. 3A). Thus, it can be concluded that liming of agricultural soils alters CUE depending on the initial soil pH and the span of the pH shift.

Our results suggest a negative relationship between CUE and liming-induced changes in soil pH at low pH (pH$_{H2O}$ = 4.5 to pH$_{H2O}$ = 7.3 at Jyndevad) and a positive relationship at high pH (pH$_{H2O}$ = 6.5 to pH$_{H2O}$ = 7.8 at Dürnast). Similarly, opposing CUE responses to anthropogenically induced pH-shifts for low (acidic to neutral) and high pH (neutral to alkaline) were reported earlier. For example, laboratory liming of an Indian arable Acrisol reduced CUE with a shift from pH$_{CaCl2}$ = 4.4 in non-limed to pH$_{CaCl2}$ = 6.6 in limed soils (Moran-Rodas et al., 2023). Furthermore, CUE declined when agricultural intensification resulted in an increase in soil pH which stayed below a threshold of pH$_{H2O}$ = 6.2, indicating a negative correlation between CUE and soil pH at low pH (Malik et al., 2018). At high pH, CUE increased along a gradient of pH$_{H2O}$ = 6.0 to pH$_{H2O}$ = 8.5 for agricultural soils after land-use change in the subarctic, where soil pH increased after conversion due to wood-ash amendment (Schroeder et al., 2022). And in the study by Malik et al. (2018), pH shifts above the pH$_{H2O}$ = 6.2 threshold increased CUE. However, the authors reported that pH increases starting from an initial soil pH higher than pH$_{H2O}$ = 6.2 where negatively correlated to CUE, indicating a zig-zag relationship along the full range. Results by Jones et al. (2019) contradict the here observed pattern. Across 970 highly weathered Australian agricultural soils, a positive relationship was found between CUE and soil pH at low pH$_{CaCl2}$ < 5.5. Above this threshold, CUE remained constant (pH$_{CaCl}$ range of all soils from 3.5 to 7.6) (Jones et al., 2019). Thus, the relationship between CUE and soil pH has previously been observed to change along pH gradients. But in contrast to the here proposed U-shaped relationship, CUE followed a zig-zag pattern (Malik et al., 2018) or increased until a threshold of pH$_{CaCl2}$ = 5.5 and then levelled off thereafter (Jones et al., 2019). Yet, a U-shaped relationship between CUE and soil pH was also found for CUE estimated by stoichiometric models for >2000 soils from a broad range of ecosystems (Sinsabaugh et al., 2016). However, to the best of our knowledge, our study is the first description of a U-shaped CUE response based on measured CUE data.

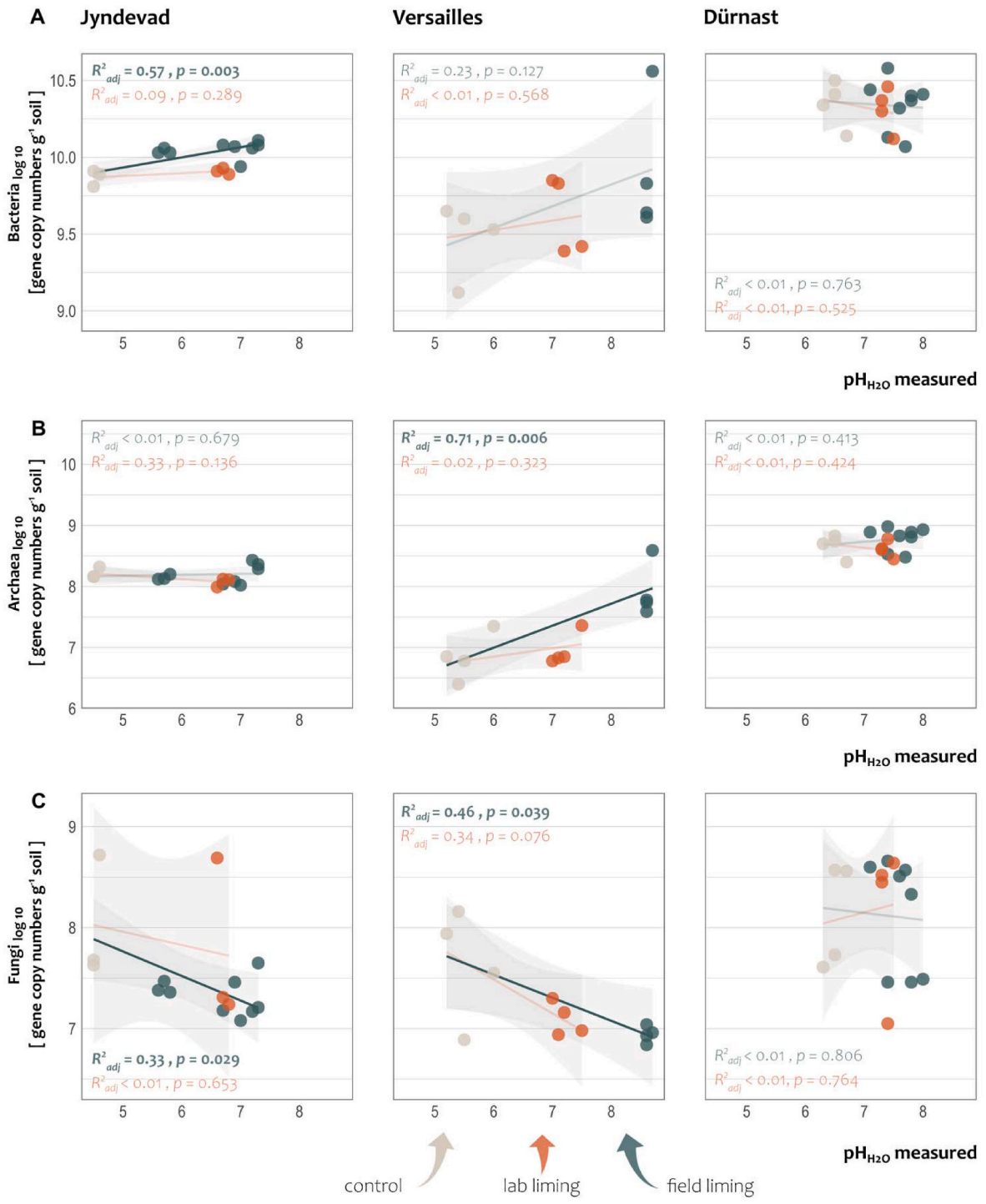

Fig. 6. Estimated abundances of **A)** bacteria, **B)** archaea and **C)** fungi given as the $\log_{10}$-transformed number of gene copies g^{-1} soil as determined by qPCR. Values are given per site, where colour indicates the control (grey) and different liming treatments (lab liming: orange; field liming: green). The liming-induced shift in soil pH was considered to have a significant effect on microbial abundance if the linear regression indicated a relationship with soil pH at $p < 0.05$.

The U-shaped relationship between CUE and soil pH is a result of the combined opposing effects of pH on absolute C_{Growth} and $C_{Respiration}$: While microbial growth seems to be lowest at near neutral pH, respiration tends to be highest, as seen from the overall pattern of z-transformed rates (Fig. S2). It has been suggested that a soil pH shift above a proposed threshold pH-value of $pH_{H2O} = 6.2$ (Malik et al., 2018) or an increase until a threshold of $pH_{CaCl2} = 5.5$ (Jones et al., 2019) might promote increases in CUE by reducing the trade-off caused by stress alleviation (e.g. H_3O^+, Al^{3+}). Despite the observed divergent CUE soil pH relationships, these values are close to the here identified threshold at $pH_{H2O} = 6.4$. This supports the conclusion of a non-linear relationship between CUE and soil pH across the entire pH range.

It should be noted that the mentioned studies by Jones et al. (2019), Malik et al. (2018), and Moran-Rodas et al. (2023) employed CUE methods with addition of labelled substrate (^{14}C-glucose, ^{13}C labelled dissolved organic C, and ^{13}C labelled litter, respectively), which may induce priming effects and is rather indicating the potential efficiency of specific substrate utilisation, whereas the ^{18}O-labelling method (used in

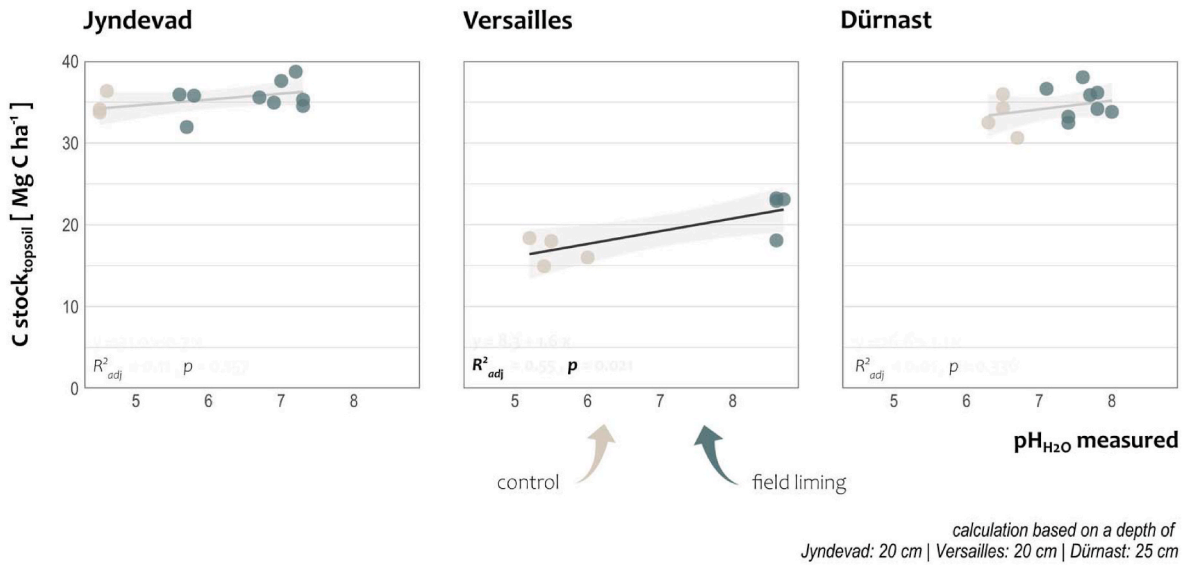

Fig. 7. Soil organic carbon stocks in topsoils (C $stock_{topsoil}$) did not increase linearly with the liming-induced shift in soil pH at Jyndevad (0–20 cm) and Dürnast (0–25 cm) but at Versailles (0–25 cm). Values are given for control soils (grey) and field liming (green) per site. Long-term liming was considered to have a significant effect by the increase in soil pH if the linear regression indicated a significant relationship at $p < 0.05$.

the present study) allows to assess the potential CUE during native (site-specific) soil organic matter decomposition (Geyer et al., 2019). However, differences in methodology may not explain divergent CUE and soil pH relationships, since studies using a similar method (Jones et al., 2019; Malik et al., 2018) show inconsistent results. Differences between studies could also be related to the availability of cations, which was recently reported to affect CUE (Horn et al., 2021; Shabtai et al., 2023). We acknowledge that three long-term field experiments may not be sufficient to infer a general pattern of the relationship between microbial CUE and soil pH, so that the pH CUE relationship is not yet fully resolved. However, our observations suggest that the first hypothesis, i.e. long-term liming promotes higher CUE, must be rejected. Liming does not promote CUE in all cases.

4.2. Potential mechanisms underlying the observed effects of liming on CUE

4.2.1. Liming effect on CUE at low pH

At low pH we expected that liming would facilitate microbial growth by the alleviation of Al^{3+}/H^{+} toxicity and overall growth condition improvement, allowing a higher fraction of resources to be directed to microbial growth instead of stress mitigation (Jones et al., 2019). Thus, it was unexpected to observe that CUE declined. Reductions in CUE with long-term liming at low pH (Jyndevad) were driven by a decline in the mass specific growth rate (i.e. specific C_{Growth}), whereas respiration increased proportionally with microbial biomass. It means that while the total amount of microbial biomass increased, the growing fraction declined. It seems reasonable to assume that such a change in the growing fraction is related to the microbial community itself and not to direct impacts of altered nutrient availability on microbial metabolism. The decline in mass specific C_{Growth} contradicts a shift towards a fast-growing copiotrophic microbial community, which could have explained the decrease in CUE, since copiotrophs are hypothesised to show lower CUE than oligotrophs (Manzoni et al., 2012; Roller and Schmidt, 2015). Microbial growth was shown to shift from fungal to bacterial dominated along a pH gradient (Rousk et al., 2010b). Further, a negative exponential relationship between the growth dominance of fungi and the microbial CUE was reported across nine different sites of different land-use types (Soares and Rousk, 2019). Therefore, we suggest that the observed reduction in CUE at low pH occurred due to shifts in fungal:bacterial growth dominance. Such shifts in growth dominance would be in line with the observed shift in the microbial community composition with long-term liming at Jyndevad toward lower fungal and higher bacterial abundances (Fig. 6). Previous findings suggest that CUE changes are directly induced by alteration of soil pH and not by pH-induced shifts in microbial community composition (Schroeder et al., 2022). However, as previously mentioned, the results of Schroeder et al. (2022) refer to higher pH range, where the underlying mechanisms may differ, and do not necessarily contradict the suggested mechanism at low pH.

4.2.2. Liming effect on CUE at high pH

At high pH ($pH_{H2O} > 6.4$), we observed that further raises in soil pH increased microbial CUE. This observed relationship between CUE and soil pH between $pH_{H2O} = 5.5$ and $pH_{H2O} = 8.5$ is likely related to factors other than alleviated stress conditions. Relevant Al^{3+}-concentrations in soil solution occur only at soil pH < 5.0 (Blume et al., 2016). Further, Al^{3+}-toxicity was shown to be relevant for CUE only at low pH < 5.5 (Jones et al., 2019). Regarding shifts in the microbial community, we observed archaeal abundance to increase with long-term liming to alkaline conditions at $pH_{H2O} = 8.5$ at Versailles. In line, the archaeal abundance was found to increase with higher soil pH (Grover et al., 2021). However, the ecological importance of archaea in microbial C cycling, and other biogeochemical processes in agroecosystems, e.g. as ammonia-oxidizer in the N-cycle, still needs to be better documented (Naitam and Kaushik, 2021; Offre et al., 2013). Besides the long-term effects of liming on archaea, fungal abundance decreased with increasing soil pH at Versailles. Changes in CUE in response to long-term and lab liming at Versailles pointed in the same direction, but specific C_{Growth} and $C_{Respiration}$ were differently affected. While the increase in CUE with long-term liming was linked to a reduction in specific $C_{Respiration}$ ($LME_{overall}$ $p_{adj} = 0.0009$), *lab liming* slightly increased microbial CUE by 16 % due to a stimulation of specific C_{Growth} ($LME_{overall}$ $p_{adj} = 0.0052$). It remains unclear whether the underlying mechanisms of immediate and long-term response of CUE to lime addition may differ. The observed trend in increasing CUE with long-term liming at Dürnast was caused by the combined slight reduction in specific $C_{Respiration}$ and increase in specific C_{Growth} at the same time. Since CO_2 solubility in water increases with soil pH, there is a risk of underestimating microbial respiration rates in alkaline soils. However, given the high headspace-to-water ratio in our incubation vessels, this effect was marginal. We conducted an error estimation (supplemental information)

and expect the highest maximum relative error of 0.11 % to occur in the Versailles *limed* treatment (Table S5), which can be neglected. No shift in microbial community with long-term liming nor lab liming was observed at Dürnast, making it an unlikely explanation for the observed trend of increases in CUE (Table 2). The observation that CUE was stimulated by both a reduction in $C_{Respiration}$ and increase in C_{Growth} indicates that changes could indeed be related to a direct metabolic response to altered nutrient availability, e.g. N or C, rather than by larger shifts in the active microbial community.

4.2.3. Direct liming effect on CUE

The addition of lime to the control soils in the laboratory induced changes in CUE similar to long-term field liming, although less pronounced, indicating that liming may alter CUE via a direct control. While differences in CUE between control and lab liming were significant at Jyndevad and Versailles, *lab liming* did not significantly alter CUE at Dürnast ($LME_{overall}$). The lack of significant response to lab liming at Dürnast is explained by the fact that at this site lab liming only induced a relatively small shift in soil pH_{H2O} from 6.5 to 7.4, i.e. to the level of the field treatment *Medium lime* which did neither significantly differ in CUE from the control soils. This stresses that the span of the lime-induced shift in soil pH is relevant for the CUE response to liming. If not corrected for lime-derived CO_2-emissions, which contributed between 20 and 70 % depending on the pH shift induced, CUE values were underestimated, highlighting the importance of accounting for the contribution of lime as CO_2 source.

We hypothesised that raising soil pH with liming would immediately increase CUE by improving growth conditions. Indeed, the shift in soil pH altered microbial CUE immediately within one week after lime addition. It can be assumed that such an immediate effect of lime-induced pH shifts on CUE may be either related to changes in the active microbial fraction or the altered availability of organic matter (e.g. desorption of dissolved organic matter from clay minerals) affecting microbial physiology. In the laboratory, we observed that lab liming increased the amount of K_2SO_4-extractable C in non-fumigated samples (Table S3, Fig. S1). K_2SO_4-extractable C is considered a proxy for the labile organic C pool (Rousk and Jones, 2010). Therefore, the observed increase in K_2SO_4-extractable C suggests that direct lime addition affected C availability. Improved labile C availability may have caused the significant increase in CUE in response to lab liming at the highly C depleted bare fallow site Versailles. We suggest that increases in available resources via pH-related shifts in sorption/desorption equilibria, as seen from K_2SO_4-extractable C, may also explain the observed stimulation of C_{mic} after laboratory lime addition. Although the observed increase in C_{mic} and K_2SO_4-extractable C concentrations supports the hypothesis that liming sustains better microbial growth conditions, we observed that CUE declined in direct response to laboratory lime addition at Jyndevad similar to long-term liming. At Jyndevad, CUE was significantly reduced by 16 % in direct response to laboratory liming as absolute respiration rate increased slightly more than absolute growth rate in comparison to control soils. Jyndevad was the only site where absolute $C_{Respiration}$ was altered by laboratory lime addition (Fig. 2), which is explained by the relatively large difference in C_{mic} between laboratory limed and control soil (Table S2). While at Jyndevad long-term liming decreased the proportion of fungi in the soil microbiome, as indicated by qPCR, this effect could not be seen in the *lab liming* treatment (within one week). The lack of community shift does not necessarily mean that growth dominance wasn't affected by direct liming. Apparently, growth rates, as limited by energy rich substrate, were insufficiently high to detect changes in the abundances within days and may have additionally be covered by the persistence of relic DNA (Carini et al., 2016).

We suggest that the response of CUE to liming is associated to shifts in the fungal:bacterial growth dominance at low pH, whereas at high pH we suggest that altered nutrient availability may be the major driver of CUE increase. The second hypothesis that CUE would immediately increase with lime addition due to facilitated growth, must also be rejected, given the divergent CUE responses.

4.3. Liming effects on C accrual

We found a significant positive effect of long-term liming on SOC stocks over all three sites (i.e. $LME_{overall}$), with higher SOC stocks at increased soil pH (Fig. 7). However, the positive relationship between SOC stock and soil pH was only found significant at Versailles (i.e. $LME_{site\text{-}wise}$), where stocks were 30 % higher in limed as compared to control plots, while at Jyndevad and Dürnast C stocks only increased by 5 % at highest liming level. In line, no significant increase in SOC stocks for the studied level of P application was found for the Jyndevad long-term experiment earlier (Abalos et al., 2020), whereas significantly higher SOC stocks in limed plots were reported previously for Versailles (Paradelo et al., 2016). However, taken together the three experiments indicated that liming supports higher SOC stocks. The net effect of liming on SOC stocks is the sum of individual effects of liming induced pH shifts and the increase in exchangeable Ca^{2+} (Paradelo et al., 2015). To assess the potential contribution of CUE to the net liming effect on SOC stocks, Fig. 8 illustrates the responses of essential factors relevant for SOC dynamics to the highest respective liming level of each site.

OC input rates (excluding the bare fallow site Versailles) increased significantly with liming (Fig. S3). While the total OC input was smaller at Jyndevad than at Dürnast, the relative increase as compared to the unlimed treatment was three times larger (Fig. 8). This is due to the high difference in OC input rate between limed and control soils at Jyndevad. Indeed, it was reported that crop growth failed occasionally in non-limed plots, likely due to Al^{3+} toxicity at the low $pH_{H2O} = 4.5$ (Azeez et al., 2020). We conclude that at Jyndevad OC input likely increased due to alleviation of Al^{3+}-toxicity. At Dürnast, control soils were already close to the optimum pH for plant growth, likely restricting the positive effect of liming on OC input in comparison to Jyndevad. Crops may still have benefited from increased soil pH, as it was shown in an earlier study that liming increased plant P availability at Dürnast (Tucher et al., 2018). Furthermore, lime addition may have affected crop growth and thus OC input by improved water balance at both sites, as we found that long-term liming increased water-holding capacity linearly with the amount of added lime at all sites (Fig. S4).

Liming increased microbial biomass (Fig. 4), which is in line with earlier findings (Abalos et al., 2020; Grover et al., 2021; Pietri and Brookes, 2008). The increase in C_{mic} likely relates to the increase in OC input at Jyndevad and Dürnast (Fig. S3). Despite a threefold increase in OC input, liming did not stimulate C_{mic} to a similar extent at Jyndevad (Fig. 8). This may be related to the fact that the growing fraction declined and CUE was reduced with lime addition, reducing the amount of OC input being directed to C_{mic}. Furthermore, we observed that K_2SO_4-extractable C concentrations of long-term limed soils were smaller as compared to control soils (Table S3), indicating a lower availability of OC likely due to Ca^{2+}-sorption with long-term liming (Römkens et al., 1996). Detailed understanding on how liming affects the availability of organic matter in agricultural soils is lacking (Kalbitz et al., 2000). However, it can be concluded that the increase in OC input not directly translates into higher C_{mic}. Given the relatively small increases in OC input with liming at Dürnast, it can be assumed that higher CUE with liming may have supported the observed increase in C_{mic} (Fig. 8). Furthermore, the increase in C_{mic}/C_{org} at Versaille suggests that the higher microbial biomass was mainly sustained by higher CUE, because OC inputs were excluded in the bare fallow experiment. Summarising, our findings suggest that C_{mic} is controlled by both organic matter availability (i.e. OC inputs and/or physicochemical protection) and CUE. We observed that liming increased the proportion of microbial biomass to total SOC, i.e. C_{mic}/C_{org} (Table 3), indicating that more microbial biomass was sustained per unit SOC. Conversely, this also means that C_{mic} increased to a larger extent than SOC stock (Fig. 8). The *in-vivo* pathway of C stabilisation may be supported by liming through its

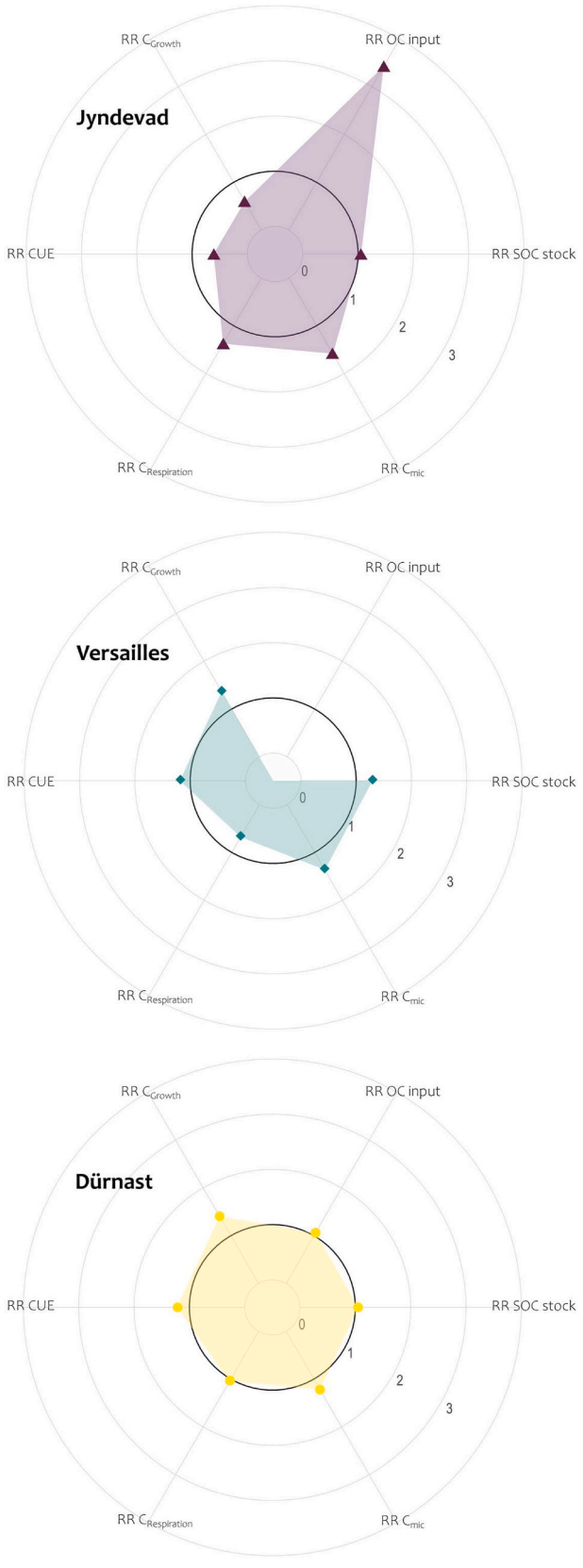

Fig. 8. Interaction of individual factors gives the net liming effect. Response ratio (RR) of soil organic C (SOC) stock, organic C (OC) input, microbial biomass C (C_{mic}), carbon use efficiency (CUE), microbial respiration rate ($C_{Respiration}$) and microbial growth rate (C_{Growth}) to the highest respective liming level at each site (Jyndevad: *lime 12*, Versailles: *limed*, Dürnast: *High lime*).

stimulating effect on C_{mic}, but remains uncertain since we did not investigate changes in MAOM fraction and associated necromass. Results by Fornara et al. (2011) indicate that liming may indeed contribute to higher MAOM formation by increased C_{mic}. However, the link between higher microbial biomass and SOC accrual is not straightforward. The increase in plant-derived OC inputs may stimulate microbial activity, thus decomposition and priming of SOC, and can therefore negatively affect C stocks (Grover et al., 2021).

CUE showed divergent liming responses as discussed above. Given that CUE determines the share between C lost as CO_2 to the atmosphere or directed to anabolism, changes in CUE with liming determine whether relatively more or less C is lost. Consequently, total respiration increased along with reduced CUE at Jyndevad, whereas respiration decreased or was unaltered with higher CUE at Versailles and Dürnast, although C_{mic} increased in all cases (Fig. 8). However, SOC stocks were not linearly correlated to CUE.

Different scenarios of how liming affects SOC dynamics were observed in this study.

Scenario one - decreasing CUE counteracts increasing inputs

At low initial soil pH, liming improved crop growth to a large extent and thus resulted in threefold increase in OC input at Jyndevad. However, the large increase in OC input was likely counterbalanced by a reduction in CUE going along with higher relative CO_2 losses during decomposition (Fig. 8). As a result, only a small proportion of 1–2 % of addition OC input was stabilised as SOC. In addition, the coarse sandy soil may be limited in C stabilisation via formation of MAOM due to its low silt and clay proportion, i.e. low mineral surface area (Abalos et al., 2020). Thus, texture may also explain the relatively low SOC formation efficiency of OC inputs as compared to Dürnast (10–20 %). However, the fact that a threefold increase in OC inputs did not result in a significant increase in SOC over 80 years is likely to be related to a concomitant decrease in microbial CUE.

Scenario two - increased OC input and CUE cause SOC accrual

At high initial soil pH, the benefit of liming for crop growth and thus OC input was much smaller. However, the sum of positive liming responses of OC input and CUE may have resulted in SOC accrual, by reducing the relative amount of C lost as CO_2 during decomposition (Fig. 8). Indeed, we observed that SOC formation efficiency was higher for *High lime* as compared to *Medium lime*, which indicates that the OC input was not the only reason for the positive trends in SOC associated with liming. In fact, *High lime* also had a 13 % higher CUE than *Medium lime* which is a strong hint towards a positive effect of CUE on C accrual. It remains unknown, how far OC stabilisation via Ca^{2+} bridges and more stable aggregates contributed to a higher SOC formation efficiency in the *High lime* treatment.

Scenario three - Increased CUE and lower bioavailability maintain stabilised SOC

The bare fallow at Versailles (i.e. no OC inputs over 89 years), has to be considered a special case, which enables the evaluation of a third, i.e. a no-input scenario. Long-term lime amendment resulted in significantly less C depletion as compared to control soils. Almost all labile C is considered depleted (Barré et al., 2010). It can thus be assumed that SOC is mostly present in the form of stabilised C and microbial biomass. Ca^{2+}-addition may have contributed to higher SOC stock by improving physical and physicochemical protection of organic matter (Paradelo et al., 2015). Indeed, limed plots at Versailles are characterised by a more aggregated structure (Paradelo et al., 2016), indicating higher Ca^{2+} bridging of minerals and organic matter. Despite higher microbial biomass and a higher SOC stock, respiration was reduced by liming, pointing towards a lower bioavailability of SOC (Fig. 8). At the same time, microbial growth and biomass were higher in the limed treatment as compared to the unlimed fallow (Fig. 8), suggesting a more efficient recycling of microbial necromass and other available C resources. For the Versailles soils, it has been shown that recycling of microbial metabolites is the primary resource for microbial communities (Nunan et al., 2015), stressing the importance of efficient necromass recycling

for C dynamics. Thus, also in this scenario the liming-induced change in CUE most likely affected C cycling in the soil.

Interestingly, the CUE observed in the C-depleted bare fallow at Versailles was very close to the assumed stoichiometric maximum CUE of 0.88 (Gommers et al., 1988). In line with this observation, CUE values were observed to increase along a depth gradient with decreasing SOC (Dămătîrcă et al. submitted). In general, it is assumed that CUE is higher with increased availability of nutrients (Manzoni et al., 2017). While C depletion may reduce resource availability, it may increase relative availability of nutrients such as N and P as compared to C-rich soils. However, we did not observe significant differences in soil C:N ratio at Versailles. Our results may suggest that severe C limitation favours efficient metabolic strategies.

Our findings suggest, that altered CUE is not the primary cause of SOC stock changes but helps to explain net effect of liming. Recently, CUE was found to be the major determinant of SOC stocks on a global scale, more than four times as important as OC inputs (Tao et al., 2023). This study used microbial explicit modelling and deep learning to retrieve major predictors of CUE and SOC stocks of approximately 57.000 soil profiles. In our study, increases in CUE by 16 % and 24 % were not significantly correlated to SOC stock changes. Our findings challenge the conclusion by Tao et al. (2023) that a relative increase in CUE by 2 % (i.e. an increase of 0.28–0.29) results in a 10 % increase in SOC stocks. The importance of CUE for SOC stock prediction found by Tao et al. (2023) may be inherent to the model and associated assumptions (He et al., 2023). Our findings and other work (He et al., 2023) point out the role of OC inputs and abiotic factors for C stocks. We found that CUE is potentially highest at acidic or alkaline pH and lowest at near neutral soil conditions, contrasting the optimal pH for plant nutrition. Thus, at both high and low initial soil pH, liming may result in contrasting responses of crop growth and microbial CUE, potentially obscuring the overall effects on SOC. Given the importance of fresh OC inputs, aiming for high CUE via alteration of soil pH would therefore counteract the aim to accrue SOC.

The microbial CUE as assessed in incubation studies represents a potential CUE under controlled conditions for samples taken at one given time point. In contrast, SOC stocks are shaped over decadal to centennial timescales. Therefore, it is extremely difficult to experimentally link changes in CUE to changes in SOC (in general and especially from single measurements). However, for the three investigated sites, the observed changes in CUE could be linked to observed trends in SOC stocks in various ways, evidencing its relevance for bulk SOC dynamics.

5. Conclusions

This study confirmed that soil pH can strongly influence CUE, following a quadratic relationship, with lowest potential CUE at near neutral soil pH. This implies that the liming effect on CUE depends on the initial soil pH and the extent of the induced pH shift. Mechanisms by which lime-induced shifts in soil pH affect CUE may differ between low and high pH and over time. At low initial soil pH, increases in pH may shift the microbial community and thereby reduce CUE. At high pH, alteration of nutrient availability may be the major driver of increases in CUE. The net effect of liming on SOC stocks is the sum of its individual effects on OC inputs, physicochemical protection of organic matter, microbial activity, and the microbial metabolic efficiency (direct and indirect controls). Further investigation should focus on the hypothesis that liming results in increased OC inputs which stimulate microbial activity and increase microbial biomass thereby supporting the slow build-up of MAOM and C accrual by microbial transformation of plant-derived C.

CRediT authorship contribution statement

Julia Schroeder: Conceptualization, Data curation, Formal analysis, Investigation, Methodology, Validation, Visualization, Writing – original draft, Writing – review & editing. **Claudia Dămătîrcă:** Data curation, Formal analysis, Investigation, Writing – review & editing. **Tobias Bölscher:** Resources, Writing – review & editing, Data curation. **Claire Chenu:** Data curation, Resources, Writing – review & editing. **Lars Elsgaard:** Data curation, Resources, Writing – review & editing. **Christoph C. Tebbe:** Data curation, Resources, Writing – review & editing. **Laura Skadell:** Data curation, Writing – review & editing. **Christopher Poeplau:** Conceptualization, Data curation, Funding acquisition, Investigation, Project administration, Writing – review & editing.

Declaration of competing interest

The authors declare the following financial interests/personal relationships which may be considered as potential competing interests: Julia Schroeder reports financial support was provided by Horizon 2020 Research and Innovation Programme.

Data availability

Data and R code used for this study are freely available at [10.5281/zenodo.10137003].

Acknowledgements

We thank the operators of the LTE areas for their tedious work and provision of data. We would like to thank the technical staff at the Thünen Institute involved in this study: Kerstin Gilke (GC), Claudia Wiese (CN), Sabine Wathsack (C_{mic}), Andrea Niemeyer (N_{mic}), Britta Müller, Karin Trescher and Jana Usarek (DNA extraction, qPCR). Special thanks to Dr. Jens Dyckmans and his colleagues at the Centre for Stable Isotope Research and Analysis of the University of Göttingen for the $\delta^{13}C$ analyses. We would also like to thank Katrin Schulz for her help with Visual MINTEQ. This study was part of the EJPSoil project, which has received funding from the European Union's Horizon 2020 research and innovation programme under grant agreement No 862695.

Appendix A. Supplementary data

Supplementary data to this article can be found online at https://doi.org/10.1016/j.soilbio.2024.109342.

References

Abalos, D., Liang, Z., Dörsch, P., Elsgaard, L., 2020. Trade-offs in greenhouse gas emissions across a liming-induced gradient of soil pH: role of microbial structure and functioning. Soil Biology and Biochemistry 150, 108006.

Allison, S.D., Wallenstein, M.D., Bradford, M.A., 2010. Soil-carbon response to warming dependent on microbial physiology. Nature Geoscience 3, 336–340.

Aphalo, P.J., 2021. Ggpmisc: Miscellaneous Extensions to 'ggplot2'. R Package Version 0.3.9.

Azeez, M.O., Christensen, J.T., Ravnskov, S., Heckrath, G.J., Labouriau, R., Christensen, B.T., Rubæk, G.H., 2020. Phosphorus in an arable coarse sandy soil profile after 74 years with different lime and P fertilizer applications. Geoderma 376, 114555.

Barré, P., Eglin, T., Christensen, B.T., Ciais, P., Houot, S., Kätterer, T., van Oort, F., Peylin, P., Poulton, P.R., Romanenkov, V., Chenu, C., 2010. Quantifying and isolating stable soil organic carbon using long-term bare fallow experiments. Biogeosciences 7, 3839–3850.

Bates, D., Mächler, M., Bolker, B., Walker, S., 2015. Fitting linear mixed-effects models using lme4. Journal of Statistical Software 67, 1–48.

Bertrand, I., Delfosse, O., Mary, B., 2007. Carbon and nitrogen mineralization in acidic, limed and calcareous agricultural soils: Apparent and actual effects. Soil Biology and Biochemistry 39, 276–288.

Biasi, C., Lind, S.E., Pekkarinen, N.M., Huttunen, J.T., Shurpali, N.J., Hyvönen, N.P., Repo, M.E., Martikainen, P.J., 2008. Direct experimental evidence for the contribution of lime to CO2 release from managed peat soil. Soil Biology and Biochemistry 40, 2660–2669.

Blume, H.-P., Brümmer, G.W., Fleige, H., Horn, R., Kandeler, E., Kögel-Knabner, I., Kretzschmar, R., Stahr, K., Wilke, B.-M., 2016. Scheffer/Schachtschabel Soil Science. Springer Berlin Heidelberg, Berlin, Heidelberg.

Bölscher, T., Wadsö, L., Börjesson, G., Herrmann, A.M., 2016. Differences in substrate use efficiency: impacts of microbial community composition, land use management, and substrate complexity. Biology and Fertility of Soils 52, 547–559.
Bölscher, T., Ågren, G.I., Herrmann, A.M., 2020. Land-use alters the temperature response of microbial carbon-use efficiency in soils – a consumption-based approach. Soil Biology and Biochemistry 140, 107639.
Burgevin, H., Hénin, S., 1939. Dix années d'expériences sur l'action des engrais sur la composition et les propriétés d'un sol de limon. Annales Agronomiques 9.
Carini, P., Marsden, P.J., Leff, J.W., Morgan, E.E., Strickland, M.S., Fierer, N., 2016. Relic DNA is abundant in soil and obscures estimates of soil microbial diversity. Nature Microbiology 2, 16242.
Conant, R.T., Ryan, M.G., Ågren, G.I., Birge, H.E., Davidson, E.A., Eliasson, P.E., Evans, S.E., Frey, S.D., Giardina, C.P., Hopkins, F.M., Hyvönen, R., Kirschbaum, M.U. F., Lavallee, J.M., Leifeld, J., Parton, W.J., Megan Steinweg, J., Wallenstein, M.D., Martin Wetterstedt, J.Å., Bradford, M.A., 2011. Temperature and soil organic matter decomposition rates - synthesis of current knowledge and a way forward. Global Change Biology 17, 3392–3404.
Dămătîrcă, C., Moretti, B., Poeplau, C., Schroeder, J., Lerda, C., Celi, L., Ciorîță, A., Pittarello, M., Zavattaro, L., Lombardi, G. (submitted). Grassland's dirty little secret: enhanced carbon stocks in permanent vs temporary grasslands are limited to the topsoil.
Fierer, N., Walsh, C.M., 2023. Can we manipulate the soil microbiome to promote carbon sequestration in croplands? PLoS Biology 21, e3002207.
Fornara, D.A., Steinbeiss, S., McNamara, N.P., Gleixner, G., Oakley, S., Poulton, P.R., Macdonald, A.J., Bardgett, R.D., 2011. Increases in soil organic carbon sequestration can reduce the global warming potential of long-term liming to permanent grassland. Global Change Biology 17, 1925–1934.
Frey, S.D., Lee, J., Melillo, J.M., Six, J., 2013. The temperature response of soil microbial efficiency and its feedback to climate. Nature Climate Change 3, 395–398.
Geyer, K.M., Dijkstra, P., Sinsabaugh, R., Frey, S.D., 2019. Clarifying the interpretation of carbon use efficiency in soil through methods comparison. Soil Biology and Biochemistry 128, 79–88.
Gommers, P.J., van Schie, B.J., van Dijken, J.P., Kuenen, J.G., 1988. Biochemical limits to microbial growth yields: an analysis of mixed substrate utilization. Biotechnology and Bioengineering 32, 86–94.
Graves, S., Piepho, H.-P., Selzer, L., , with help from, Dorai-Raj, Sundar, 2019. multcompView: Visualizations of Paired Comparisons. R package version 0.1-8.
Grover, S.P., Butterly, C.R., Wang, X., Gleeson, D.B., Macdonald, L.M., Tang, C., 2021. Liming and priming: the long-term impact of pH amelioration on mineralisation may negate carbon sequestration gains. Soil Security 3, 100007.
He, X., Abramoff, R., Abs, E., Georgiou, K., Zhang, H., Goll, D.S., 2023. Contribution of carbon inputs to soil carbon accumulation cannot be neglected, p. 9. https://doi.org/10.1101/2023.07.17.549330.
Hemkemeyer, M., Christensen, B.T., Martens, R., Tebbe, C.C., 2015. Soil particle size fractions harbour distinct microbial communities and differ in potential for microbial mineralisation of organic pollutants. Soil Biology and Biochemistry 90, 255–265.
Holland, J.E., White, P.J., Glendining, M.J., Goulding, K.W.T., McGrath, S.P., 2019. Yield responses of arable crops to liming - an evaluation of relationships between yields and soil pH from a long-term liming experiment. European Journal of Agronomy: the journal of the European Society for Agronomy 105, 176–188.
Horn, E.L., Cooledge, E.C., Jones, D.L., Hoyle, F.C., Brailsford, F.L., Murphy, D.V., 2021. Addition of base cations increases microbial carbon use efficiency and biomass in acidic soils. Soil Biology and Biochemistry 161, 108392.
Hothorn, T., Bretz, F., Westfall, P., 2008. Simultaneous inference in general parametric models. Biometrical Journal. Biometrische Zeitschrift 50, 346–363.
Hyvönen, R., Ågren, G.I., Bosatta, E., 1998. Predicting long-term soil carbon storage from short-term information. Soil Science Society of America Journal 62, 1000–1005.
IUSS Working Group WRB, 2015. WRB. 2015. World reference base for soil resources 2014, update 2015. In: International Soil Classification System for Naming Soils and Creating Legends for Soil Maps. World Soil Resources Reports No. 106. FAO, Rome.
Jacobs, A., Poeplau, C., Weiser, C., Fahrion-Nitschke, A., Don, A., 2020. Exports and inputs of organic carbon on agricultural soils in Germany. Nutrient Cycling in Agroecosystems 118, 249–271.
Joergensen, R.G., 1996. The fumigation-extraction method to estimate soil microbial biomass: Calibration of the kEC value. Science of the Total Environment 28, 25–31.
Jones, D.L., Cooledge, E.C., Hoyle, F.C., Griffiths, R.I., Murphy, D.V., 2019. pH and exchangeable aluminum are major regulators of microbial energy flow and carbon use efficiency in soil microbial communities. Soil Biology and Biochemistry 138, 107584.
Kalbitz, K., Solinger, S., Park, J.-H., Michalzik, B., Matzner, E., 2000. Controls on the dynamics of dissolved organic matter in soils: a review. Soil Science 165, 277–304.
Kallenbach, C.M., Wallenstein, M.D., Schipanksi, M.E., Grandy, A.S., 2019. Managing agroecosystems for soil microbial carbon use efficiency: ecological unknowns, potential outcomes, and a path forward. Frontiers in Microbiology 10, 1146.
Keiblinger, K.M., Hall, E.K., Wanek, W., Szukics, U., Hämmerle, I., Ellersdorfer, G., Böck, S., Strauss, J., Sterflinger, K., Richter, A., Zechmeister-Boltenstern, S., 2010. The effect of resource quantity and resource stoichiometry on microbial carbon-use-efficiency. FEMS Microbiology Ecology 73, 430–440.
Kuznetsova, A., Brockhoff, P.B., Christensen, R.H.B., 2017. lmerTest package: tests in linear mixed effects models. Journal of Statistical Software 82, 1–26.
Lauber, C.L., Strickland, M.S., Bradford, M.A., Fierer, N., 2008. The influence of soil properties on the structure of bacterial and fungal communities across land-use types. Soil Biology and Biochemistry 40, 2407–2415.
Lenth, R.V., 2021. Emmeans: Estimated Marginal Means, Aka Least-Squares Means. R package version 1.5.4.
Liang, C., Schimel, J.P., Jastrow, J.D., 2017. The importance of anabolism in microbial control over soil carbon storage. Nature Microbiology 2, 17105.
Liang, C., Amelung, W., Lehmann, J., Kästner, M., 2019. Quantitative assessment of microbial necromass contribution to soil organic matter. Global Change Biology 25, 3578–3590.
Malik, A.A., Puissant, J., Buckeridge, K.M., Goodall, T., Jehmlich, N., Chowdhury, S., Gweon, H.S., Peyton, J.M., Mason, K.E., van Agtmaal, M., Blaud, A., Clark, I.M., Whitaker, J., Pywell, R.F., Ostle, N., Gleixner, G., Griffiths, R.I., 2018. Land use driven change in soil pH affects microbial carbon cycling processes. Nature Communications 9, 3591.
Manzoni, S., Čapek, P., Mooshammer, M., Lindahl, B.D., Richter, A., Šantrůčková, H., 2017. Optimal metabolic regulation along resource stoichiometry gradients. Ecology Letters 20, 1182–1191.
Manzoni, S., Taylor, P., Richter, A., Porporato, A., Agren, G.I., 2012. Environmental and stoichiometric controls on microbial carbon-use efficiency in soils. New Phytologist 196, 79–91.
Martin, K.J., Rygiewicz, P.T., 2005. Fungal-specific PCR primers developed for analysis of the ITS region of environmental DNA extracts. BMC Microbiology 5, 28.
Mooshammer, M., Wanek, W., Zechmeister-Boltenstern, S., Richter, A., 2014. Stoichiometric imbalances between terrestrial decomposer communities and their resources: mechanisms and implications of microbial adaptations to their resources. Frontiers in Microbiology 5, 22.
Moran-Rodas, V.E., Joergensen, R.G., Wachendorf, C., 2023. Does liming improve microbial carbon use efficiency after maize litter addition in a tropical acidic soil? Biology and Fertility of Soils.
Naitam, M.G., Kaushik, R., 2021. Archaea: An agro-ecological perspective. Current Microbiology 78, 2510–2521.
Neuwirth, E., 2014. RColorBrewer: ColorBrewer Palettes. R Package Version 1, pp. 1–2.
Nunan, N., Lerch, T.Z., Pouteau, V., Mora, P., Changey, F., Kätterer, T., Giusti-Miller, S., Herrmann, A.M., 2015. Metabolising old soil carbon: simply a matter of simple organic matter? Soil Biology and Biochemistry 88, 128–136.
Offre, P., Spang, A., Schleper, C., 2013. Archaea in biogeochemical cycles. Annual Review of Microbiology 67, 437–457.
Paradelo, R., Virto, I., Chenu, C., 2015. Net effect of liming on soil organic carbon stocks: a review. Agriculture, Ecosystems & Environment 202, 98–107.
Paradelo, R., van Oort, F., Barré, P., Billiou, D., Chenu, C., 2016. Soil organic matter stabilization at the pluri-decadal scale: insight from bare fallow soils with contrasting physicochemical properties and macrostructures. Geoderma 275, 48–54.
Pietri, A.J., Brookes, P.C., 2008. Relationships between soil pH and microbial properties in a UK arable soil. Soil Biology and Biochemistry 40, 1856–1861.
Posit team, 2022. RStudio. Integrated Development Environment for R. Posit Software, PBC, Boston, MA.
R Core Team, 2020. R: A Language and Environment for Statistical Computing. R Foundation for Statistical Computing, Vienna, Austria.
Roller, B.R.K., Schmidt, T.M., 2015. The physiology and ecological implications of efficient growth. The ISME Journal 9, 1481–1487.
Römkens, P.F., Bril, J., Salomons, W., 1996. Interaction between Ca^{2+} and dissolved organic carbon: implications for metal mobilization. Applied Geochemistry 11, 109–115.
Rousk, J., Bååth, E., Brookes, P.C., Lauber, C.L., Lozupone, C., Caporaso, J.G., Knight, R., Fierer, N., 2010a. Soil bacterial and fungal communities across a pH gradient in an arable soil. The ISME Journal 4, 1340–1351.
Rousk, J., Brookes, P.C., Bååth, E., 2010b. Investigating the mechanisms for the opposing pH relationships of fungal and bacterial growth in soil. Soil Biology and Biochemistry 42, 926–934.
Rousk, J., Jones, D.L., 2010. Loss of low molecular weight dissolved organic carbon (DOC) and nitrogen (DON) in H2O and 0.5 M K2SO4 soil extracts. Soil Biology and Biochemistry 42, 2331–2335.
Rudis, B., 2020. Hrbrthemes: Additional Themes, Theme Components and Utilities for 'ggplot2. https://CRAN.R-project.org/package=hrbrthemes.
Saifuddin, M., Bhatnagar, J.M., Segrè, D., Finzi, A.C., 2019. Microbial carbon use efficiency predicted from genome-scale metabolic models. Nature Communications 10, 3568.
Schimel, J.P., Schaeffer, S.M., 2012. Microbial control over carbon cycling in soil. Frontiers in Microbiology 3, 348.
Schroeder, J., Kammann, L., Helfrich, M., Tebbe, C.C., Poeplau, C., 2021. Impact of common sample pre-treatments on key soil microbial properties. Soil Biology and Biochemistry 160, 108321.
Schroeder, J., Peplau, T., Pennekamp, F., Gregorich, E., Tebbe, C.C., Poeplau, C., 2022. Deforestation for agriculture increases microbial carbon use efficiency in subarctic soils. Biology and Fertility of Soils. https://doi.org/10.1007/s00374-022-01669-2.
Shabtai, I.A., Wilhelm, R.C., Schweizer, S.A., Höschen, C., Buckley, D.H., Lehmann, J., 2023. Calcium promotes persistent soil organic matter by altering microbial transformation of plant litter. Nature Communications 14, 6609.
Sinsabaugh, R.L., Turner, B.L., Talbot, J.M., Waring, B.G., Powers, J.S., Kuske, C.R., Moorhead, D.L., Follstad Shah, J.J., 2016. Stoichiometry of microbial carbon use efficiency in soils. Ecological Monographs 86, 172–189.
Soares, M., Rousk, J., 2019. Microbial growth and carbon use efficiency in soil: links to fungal-bacterial dominance, SOC-quality and stoichiometry. Soil Biology and Biochemistry 131, 195–205.
Spohn, M., Klaus, K., Wanek, W., Richter, A., 2016. Microbial carbon use efficiency and biomass turnover times depending on soil depth - implications for carbon cycling. Soil Biology and Biochemistry 96, 74–81.
Tao, F., Huang, Y., Hungate, B.A., Manzoni, S., Frey, S.D., Schmidt, M.W.I., Reichstein, M., Carvalhais, N., Ciais, P., Jiang, L., Lehmann, J., Wang, Y.-P., Houlton, B.Z., Ahrens, B., Mishra, U., Hugelius, G., Hocking, T.D., Lu, X., Shi, Z.,

Viatkin, K., Vargas, R., Yigini, Y., Omuto, C., Malik, A.A., Peralta, G., Cuevas-Corona, R., Di Paolo, L.E., Luotto, I., Liao, C., Liang, Y.-S., Saynes, V.S., Huang, X., Luo, Y., 2023. Microbial carbon use efficiency promotes global soil carbon storage. Nature 618, 981–985.

Truog, E., 1943. The Liming of Soils. USDA Yearbook of Agriculture 1943-1947, pp. 566–576.

Tucher, S. von, Hörndl, D., Schmidhalter, U., 2018. Interaction of soil pH and phosphorus efficacy: long-term effects of P fertilizer and lime applications on wheat, barley, and sugar beet. Ambio 47, 41–49.

Vance, E.D., Brookes, P.C., Jenkinson, D.S., 1987. An extraction method for measuring soil microbial biomass C. Soil Biology and Biochemistry 19, 703–707.

Wang, Y., Yao, Z., Zhan, Y., Zheng, X., Zhou, M., Yan, G., Wang, L., Werner, C., Butterbach-Bahl, K., 2021. Potential benefits of liming to acid soils on climate change mitigation and food security. Global Change Biology 27, 2807–2821.

Wickham, H., Averick, M., Bryan, J., Chang, W., McGowan, L., François, R., Grolemund, G., Hayes, A., Henry, L., Hester, J., Kuhn, M., Pedersen, T., Miller, E., Bache, S., Müller, K., Ooms, J., Robinson, D., Seidel, D., Spinu, V., Takahashi, K., Vaughan, D., Wilke, C., Woo, K., Yutani, H., 2019. Welcome to the tidyverse. Journal of Open Source Software 4, 1686.

Wilke, C.O., 2020. Cowplot: Streamlined Plot Theme and Plot Annotations for 'ggplot2'. R Package version 1.1.1.

Yu, Y., Lee, C., Kim, J., Hwang, S., 2005. Group-specific primer and probe sets to detect methanogenic communities using quantitative real-time polymerase chain reaction. Biotechnology and Bioengineering 89, 670–679.